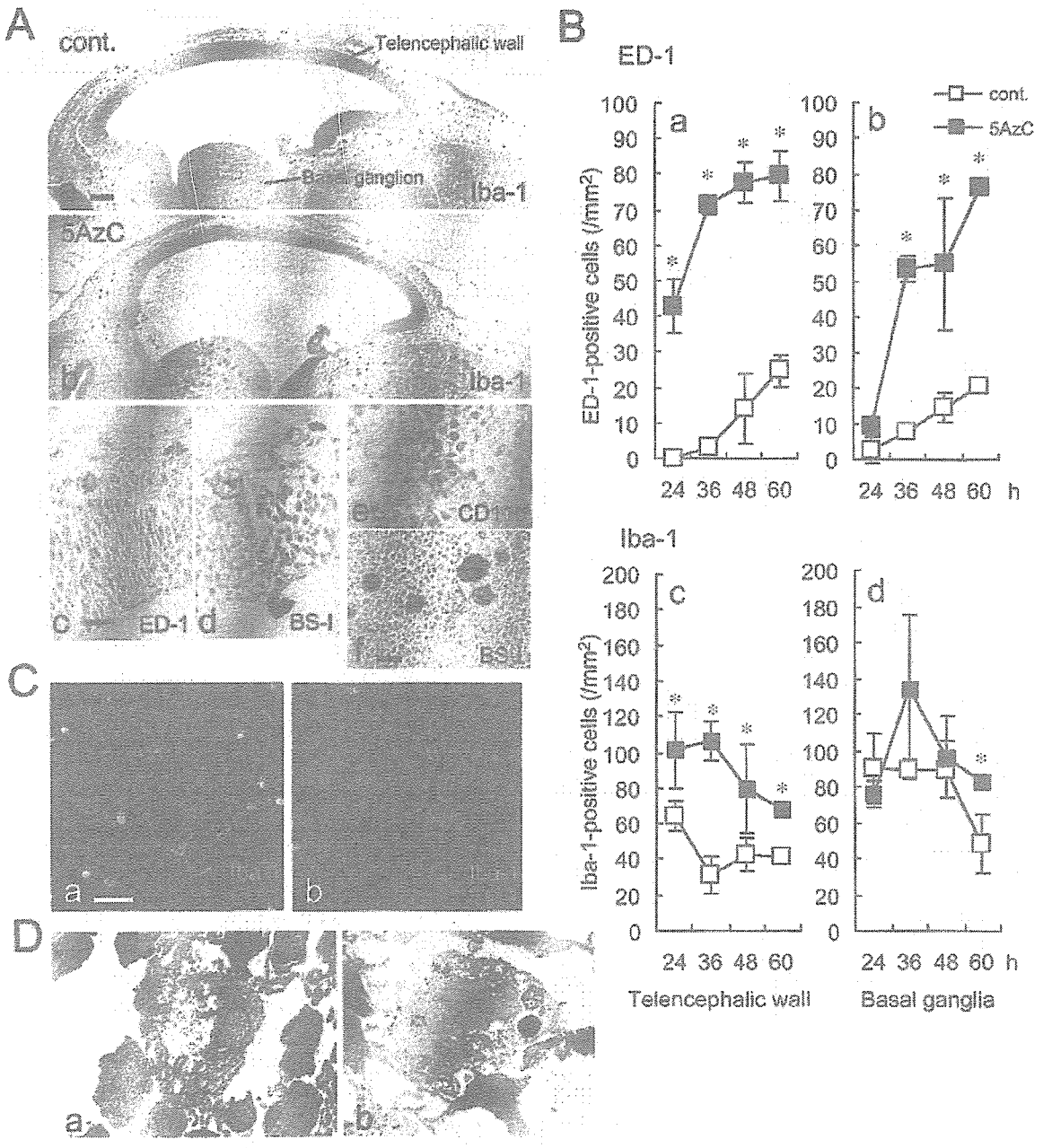

FIG. 3. Infiltration and activation of microglia in the 5-azacytidine (5AzC)-treated telencephalon. (A) Detection of microglia with several immunohistochemical markers (a, control; b–f, 5AzC-treated) at 36 h after treatment. (a and b) Iba-1; (e) ED-1; (d and f) BS-I; (e) CD11b. (a and b) Telencephalon (telencephalic wall and basal ganglion); (c and d) telencephalic wall; (e and f) basal ganglia. Scale bars: 150 μm (a and b) and 50 μm (c–f). (B) Microglial cell index. (a and b) ED-1- and (c and d) Iba-1-positive microglia were counted in control (white square) and 5AzC-treated (black square) telencephalic wall (a and c) and basal ganglia (b and d). *$P < 0.05$: significantly different from the control group (Student's *t*-test). The number of marker-positive cells increased except for Iba-1-positive cells in basal ganglia (d). (C) Double staining of Iba-1 (green) and ED-1 (red) in control (a) and 5AzC-treated (b) basal ganglia at 36 h. Iba-1-positive ramified microglia were observed in control tissue (a). In 5AzC-damaged tissue, activated amoeboid microglial cells expressed both Iba-1 and ED-1 (b). *Blood cells that were non-specifically labeled. Scale bar, 50 μm. (D) Electron micrograph with lectin (BS-I) staining. Dendritic or spindle cell in control (a) and a rounded cell that has phagocytosed apoptotic cells in the 5AzC-treated telencephalon (b). Lectin staining in the membrane is shown as a black signal.

described in Materials and methods, 535 genes were identified (236 genes increased and 299 genes decreased), of which 317 were expressed sequence tags (ESTs). Genes whose expression showed a greater than 1.5-fold increase or decrease are shown in Table 1. Genes categorized by GenMAPP as important in glial cells, inflammation (response to wounds), the extracellular matrix, glycolysis and neural development were found to be up-regulated in our microarray analysis (Table 1). Real-time PCR was then used to confirm the mRNA expression levels of several genes whose expression levels were significantly altered in the DNA microarray analysis.

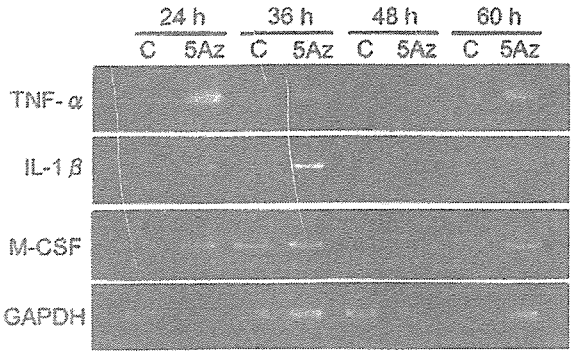

FIG. 4. Expression of cytokines important in the induction, proliferation and activation of microglial cells. C, control group; 5Az, 5-azacytidine-treated group. Levels of tumor necrosis factor (TNF)-α, interleukin (IL)-1β and M-CSF mRNA were detected by RT-polymerase chain reaction. Their expression was elevated between 24 and 60 h. Glyceraldehyde-3-phosphate dehydrogenase (GAPDH) was included as an internal control.

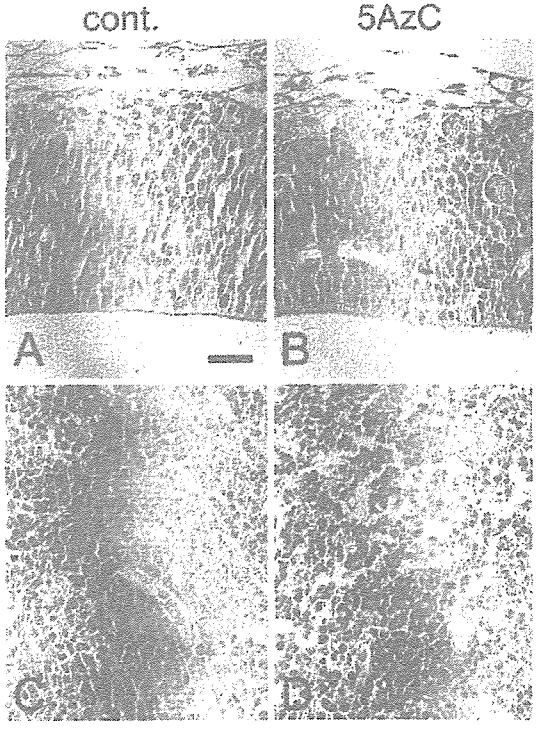

FIG. 5. Glial fibrillary acidic protein-positive astrocytes were not observed in control (A and C) and 5-azacytidine (5AzC)-treated (B and D) telencephalon at 36 h. (A and B) Telencephalic wall; (C and D) basal ganglia. Scale bar, 50 μm.

The microglial gene marker *Iba-1* was up-regulated at 24 h. This is confirmed by our immunohistochemical results of an increase in Iba-1-positive microglia in the 5AzC-treated group (Fig. 1A). Other markers of cells from macrophage lineages, *Lgals3/galectin3*, *Mif* and *osteopontin* (Walther *et al.*, 2000; Imai & Kohsaka, 2002; Calandra & Roger, 2003; Sano *et al.*, 2003; Choi *et al.*, 2004), were also up-regulated between 24 and 36 h (Table 1). The elevated expression was confirmed by real-time PCR (Fig. 6A). We detected osteopontin staining in phagocytotic microglial cells that coexpressed ED-1 (Fig. 6B). Furthermore, various genes related to response to wounds (inflammation) were up-regulated from 24 to 36 h (Table 1), suggesting that, even in the developing brain, the inflammatory response is induced by injury. Indeed, we detected elevated expression of three cytokines, *IL-1β*, *M-CSF* and *TNF-α*, that are related to inflammation and microglial activation, as mentioned above (Fig. 4). We could not detect the up-regulation of these cytokines in the DNA microarray analysis because *IL-1β* and *M-CSF* were not present in the microarray used in this study, and the expression of *TNF-α* was too low to evaluate.

The expression of genes involved in the regulation of the extracellular matrix and glycolysis was elevated between 24 and 48 h in the 5AzC-treated group (Table 1). Confirming our microarray results with real-time PCR, we show the up-regulation of *P4ha1*, a gene coding for an enzyme involved in collagen synthesis, and *Pkm2*, encoding a glycolytic enzyme (Fig. 6, Ca and Cb), which supports the microarray data showing that these genes were changed by 5AzC treatment. The expression of genes related to neural development was also changed between 24 and 48 h (Table 1). Confirming our microarray results with real-time PCR, we show that the expression of *Fgf15*, a growth factor important for brain development, was also elevated with real-time PCR (Fig. 6, Cc).

The expression of genes involved in proliferation, cell cycle control and apoptosis was also changed between 24 and 48 h (Table 1). These changes may be related to the cell cycle alterations after 5AzC treatment or may be important in the recovery of proliferation.

Discussion

Extrinsic stresses can negatively affect brain development. Treatment with cytotoxic chemicals leads to apoptotic cell death in embryonic brains and brain malformation in neonatal pups. However, the underlying process between these two stages is largely unknown. In the present study, we found that the developmental process seems to continue after injury, as was shown by our histopathology work (Fig. 1) and analysis of cell cycle kinetics (Fig. 2), indicating that the fetal brain maintains the capacity for repair and recovery toward tissue damage. Our results also suggest that damage in the developing brain initiates regeneration more easily than in adults. Although the adult brain can reproduce neurons, astrocytes and oligodendrocytes after brain injury (Magavi *et al.*, 2000; Doetsch, 2003; Picard-Riera *et al.*, 2004), the degree of regeneration is not significant. However, regeneration occurs rapidly after damage in the developing brain (Shimada & Langman, 1970; Houle & Das, 1983; Oyanagi *et al.*, 1998), which is consistent with our results. After an injury, the plasticity seen in embryonic brains appears greater than that observed in adult brains. This is possibly due to greater proliferation of neural progenitor cells (Fig. 2) and the lack of astrocytic responses (Fig. 5) in the embryonic brain, as discussed later. Thus, our experimental model may offer important information on the mechanisms of brain regeneration.

Here we show that brain injury stimulated microglia to participate in the repair process, at least, by clearing dead cells. These microglia could have originated intrinsically, as shown in Fig. 3C that microglia changed their morphology from quiescent (ramified) to activated (amoeboid) type. Following this activation process, microglial cells seemed to express ED-1 as previously reported (Milligan *et al.*, 1991). Alternatively, microglia infiltrated from the surrounding mesenchymal areas, blood vessels or ventricles, as their presence near the pia mater of the telencephalic wall suggests (Fig. 3A). Indeed, these tissues are the sources of the monocytes and hematopoietic cells that eventually form microglia (Sorokin *et al.*, 1992; Cuadros & Navascues, 1998;

TABLE 1. Gene expression changes during the repair period of the rat fetal telencephalon after 5-azacytidine treatment

Accession no.	Genes	24 h	36 h	48 h
Glial cell				
NM_017196.1	Iba-1/allograft inflammatory factor 1 (Aif1)	1.85 ± 0.58	–	
NM_031832.1	Lectin, galactose binding, soluble 3 (Lgals3)/galectin-3/Mac2	1.85 ± 0.31	3.42 ± 1.1	–
NM_021770.2	Oligodendrocyte transcription factor 1 (Olig1)		1.83 ± 0.47	–
AF265360.1	GLAST-1a/solute carrier family 1, member 3 (Slc1a3)	–	1.77 ± 0.02	1.61 ± 0.38
Inflammation/response to wounds				
AI169104	Platelet factor 4 (PF4)/small inducible cytokine sub-family B, member 4 (Scyb4)/Cxcl4	1.71 ± 0.08		
NM_012889.1	Vascular cell adhesion molecule 1 (Vcam1)	−1.78 ± 0.07	−1.85 ± 0.24	–
AB001382.1	Osteopontin/secreted phosphoprotein 1 (Spp1)	–	2.30 ± 0.43	–
NM_031051.1	Macrophage migration inhibitory factor (Mif)	–	1.68 ± 0.03	–
NM_053843.1	Fc receptor, IgG, low-affinity III (Fcgr3)	–	1.67 ± 0.06	–
AI411618	ESTs, weakly similar to complement c1q sub-component, B chain precursor (*Rattus norvegicus*)	–	1.59 ± 0.03	–
NM_012512.1	Beta-2-microglobulin (B2m)		1.55 ± 0.16	–
BM383427	Interleukin 6 signal transducer (Il6st)/gp130 transducer chain (gp130)	–	–	1.51 ± 0.01
BI285183	Thymus cell surface antigen (Thy1)	–	–	−1.72 ± 0.85
BE111083	ESTs, highly similar to complement-activating component of RA-reactive factor precursor (Crar; *Mus musculus*)	–	–	−1.51 ± 0.14
Extracellular matrix				
BM390457	TGF-beta masking protein large sub-unit (Ltbp1)	2.04 ± 0.52	–	–
NM_024400.1	A disintegrin and metalloproteinase with thrombospondin motifs 1 (Adamts1)	1.67 ± 0.06	–	–
BI274401	Prolyl 4-hydroxylase alpha sub-unit (P4ha1)	1.50 ± 0.05	–	–
AF305418.1	Type II collagen (Col2a1)			1.71 ± 0.21
BE111752	ESTs, highly similar to procollagen alpha 1 (IV) precursor (*Mus musculus*)		–	1.65 ± 0.17
AI171185	Hyaluronan-mediated motility receptor (Hmmr/Rhamm)	–	–	1.51 ± 0.02
AI179127	Small proteoglycan I/biglycan (Bgn)/bone cartilage proteclycan I precursor	–	–	−1.56 ± 0.47
Glycolysis				
BM389769	Highly similar to 6-phosphofructokinase (*Rattus norvegicus*)	1.85 ± 0.64	–	–
NM_030834.1	Monocarboxylate transporter (Mct3)/Slc16a8	2.22 ± 0.07	1.90 ± 0.26	
AI548699	ESTs, highly similar to galactokinase (*Mus musculus*)		1.84 ± 0.55	–
NM_013190.1	Phosphofructokinase, liver, B-type (Pfkl)	–	1.74 ± 0.21	–
NM_017025.1	Lactate dehydrogenase A (Ldha)	–	1.68 ± 0.45	–
BI283882	ESTs, highly similar to glucose-6-phosphate isomerase (*Mus musculus*)	–	1.63 ± 0.29	
NM_053297.1	Pyruvate kinase 3 (Pkm2)/pyruvate kinase, isozymes M1/M2	–	1.55 ± 0.03	–
Neural development				
NM_130753.1	Fibroblast growth factor 15 (Fgf15)	1.73 ± 0.25	–	–
BI274355	Weakly similar to neuronal olfactomedin-related ER localized protein precursor (Nomr; *Rattus norvegicus*)/noelin/olfactomedin 1 (Olfm1)/pancortin	1.61 ± 0.04	–	–
NM_019161.1	Cadherin 22 (Cdh22)	2.06 ± 0.10	2.37 ± 0.6	–
NM_053744.1	Delta-like homolog (Dlk1)/Pref-1	1.60 ± 0.13	2.08 ± 0.70	1.85 ± 0.11
J02582	Apolipoprotein E (ApoE)		1.50 ± 0.06	–
NM_053429.1	Fibroblast growth factor receptor 3 (Fgfr3)	–	–	1.59 ± 0.19
NM_030856.1	Neuronal leucine-rich repeat protein-3 (Lrrn3)	−1.62 ± 0.21	–	–
M55292.1	Neural receptor protein-tyrosine kinase (TrkB)	−1.56 ± 0.06	–	–
NM_024383.1	Hairy and enhancer of split 5 (Hes5)	−1.53 ± 0.13		
AW144823	ESTs, highly similar to Sort1.A precursor (sortilin-related receptor precursor) (*Mus musculus*)		−1.57 ± 0.14	
NM_053346.1	Neuritin (Nrn)	–	−1.51 ± 0.09	–
BG668493	Superior cervical ganglia, neural specific 10 (Segn10)/stathmin-like 2 (Stmn2)	–	–	−1.54 ± 0.38
NM_053654.1	Platelet-activating factor acetylhydrolase, isoform 1b, alpha1 sub-unit (Pafah1b3)	–	–	−1.53 ± 0.45
Cell cycle/proliferation				
NM_012588.1	Insulin-like growth factor-binding protein (Igfbp3)	2.30 ± 0.43	–	–
NM_133298.1	Glycoprotein (transmembrane) nmb (Gpnmb)/osteoactivin	3.03 ± 0.15	3.16 ± 0.74	3.41 ± 0.10
NM_012760.1	Lost on transformation 1 (Lot1)	–	1.94 ± 0.07	1.98 ± 0.15
M86708.1	Inhibitor of DNA binding (Id1)	–	1.65 ± 0.29	
AI714002	ESTs, moderately similar to cell proliferation antigen Ki-67 (*Mus musculus*)			1.58 ± 0.19
AW533924	Exportin 1 (Xpo1/Crm1, yeast, homolog)			1.52 ± 0.26
AA848420	ESTs, highly similar to uracil-DNA glycosylase precursor (Ung; *Mus musculus*)	−2.01 ± 0.2	–	–
AI599423	ESTs, highly similar to growth arrest and DNA-damage-inducible protein (Gadd45 gamma; *Rattus norvegicus*)	−1.91 ± 0.05	–	–
NM_019348.1	Somatostatin receptor sub-type 2 (Sstr2)	−1.62 ± 0.01	–	–
AI412150	ESTs, weakly similar to DNA-binding protein inhibitor (Id2; *Rattus norvegicus*)	−1.57 ± 0.12		
AY043246.1	Regulator of G-protein signaling 2 (Rgs2)	−1.53 ± 0.07		
NM_031762.1	Cyclin-dependent kinase inhibitor 1B (p27, Kip1) (Cdkn1b)	–	−1.63 ± 0.23	–
BE113079	ESTs, weakly similar to nucleolin (Nucl; *Rattus norvegicus*)	–	–	−1.55 ± 0.22
Apoptosis				
NM_133561.1	Brain protein 44-like (Brp44l)/apoptosis-regulating basic protein	–	–	−1.66 ± 0.62
AI102437	Zinc finger protein RP-8 (*Rattus norvegicus*)/programmed cell death protein 2			−1.63 ± 0.40
AF441118.1	BNIP3L protein (Bnip3l)/Bcl2	–	–	−1.51 ± 0.22

Fold change is presented as the mean ± SD of two arrays. Genes that showed a greater than 1.5 × increase or decrease are shown.

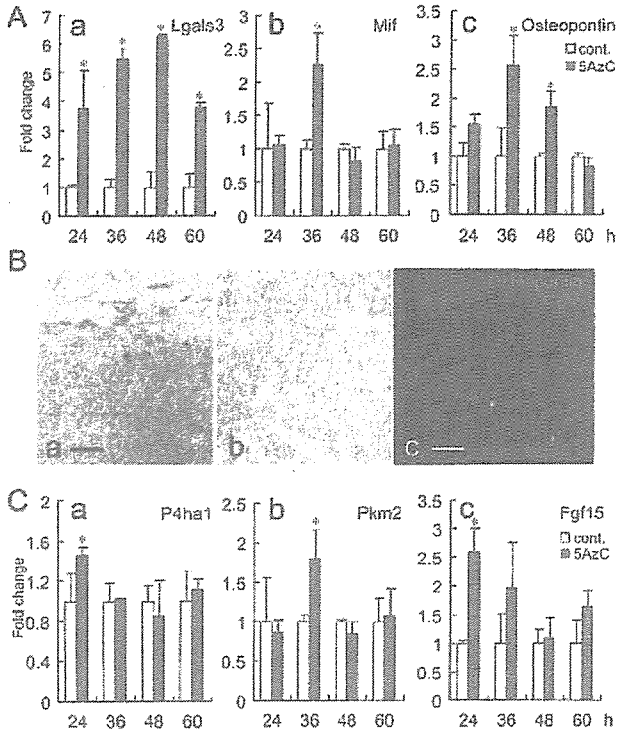

FIG. 6. The expression of genes during the repair period. (A) The expression of genes related to microglia and inflammatory responses (responses to wounding). mRNA levels of Lgals3 (a), Mif (b) and osteopontin (c), which were up-regulated in the DNA microarray analysis (Table 1), were detected by real-time polymerase chain reaction (PCR). White bar, control; grey bar, 5-azacytidine (5AzC)-treated group. Fold change relative to the control is represented as the mean ± SD of three dams. Increases in expression were consistent with the results of the DNA microarray analysis (Table 1). $^{*}P < 0.05$; significantly different from control (Student's *t*-test). (B) Osteopontin-labeled microglia in the 5AzC-treated telencephalon. (a) Telencephalic wall; (b and c) basal ganglia; 36 h after 5AzC treatment. Microglial cells were double-labeled for osteopontin (green) and ED-1 (red) (c). *Blood cells that were non-specifically labeled. Scale bar, 50 μm. (C) Expression of genes important in the extracellular matrix, glycolysis and neural development. The expression of P4ha1 (a, extracellular matrix), Pkm2 (b, glycolysis) and Fgf15 (c, neural development) was examined by real-time PCR. The representations are similar to those in A.

Kaur *et al.*, 2001), although some studies indicate that microglia can also arise partly from a neuroepithelial lineage (Cuadros & Navascues, 1998).

We further identified many up-regulated genes which indicate the presence and activation of microglial cells by using PCR and DNA microarrays. Iba-1 and Lgals3/galectin3 are both expressed in phagocytotic cells (Walther *et al.*, 2000; Imai & Kohsaka, 2002; Sano *et al.*, 2003), indicating that infiltrating microglia express these genes. Indeed, the number of Iba-1-positive microglia increased dramatically after injury (Fig. 3, Ab and Bc). Some genes involved in inflammation were also up-regulated during the repair process, suggesting that neural cells have a capacity to respond to damage and to initiate the repair process, followed by the activation of microglia. Osteopontin is expressed on amoeboid microglia in the developing brain, and is important in regulating migration and phagocytosis (Choi *et al.*, 2004). Here we found that the expression of *osteopontin* mRNA was up-regulated and that protein production was detected in phagocytotic amoeboid microglia (Fig. 6B). Brain damage induced by etylnitrosourea (a DNA-damaging agent) also leads to up-regulation of *osteopontin* during the recovery phase (Katayama *et al.*, 2005b), suggesting that osteopontin may play an important role in the repair of the developing brain. In addition, we found increased expression levels of three cytokines involved in the activation of microglial cells, *TNF-α*, *IL-1β* and *M-CSF* (Fig. 4), as well as increases of *Mif* (Table 1 and Fig. 6, Ab), a cytokine with proinflammatory effects (Calandra & Roger, 2003). The respective genes play roles in the induction, proliferation and activation of microglia (Nakajima & Kohsaka, 2001; Hanisch, 2002), and their expression is up-regulated by cyclophosphamide-induced injury to fetal brains (Hao *et al.*, 2001a). TNF-α is expressed in microglia and neural progenitor cells, and colony stimulating factor 1 receptor (CSF-1R), encoding an M-CSF receptor, in microglial cells (Hao *et al.*, 2001a,b, 2002). These reports indicate the importance of these cytokines for activating microglial cells in the developing brain. It is known that microglia release two types of opposing signaling molecules, cytotoxins and neurotrophic factors (Nakajima & Kohsaka, 2001), so further investigation of microglial function in this model is needed to clarify their role except for phagocytosing dead cells.

Moreover, we found elevated levels of markers for two other types of glial cell, oligodendrocytes and astrocytes. The expressions of *Olig-1* (Zhou *et al.*, 2000) and *Fgfr3* (Bansal *et al.*, 2003), markers of oligodendrocyte precursors, were elevated, although their role in our study remains unclear. Glast-1 is a glutamate transporter whose gene is expressed in astrocytes in the adult brain as well as on neural progenitor cells (radial glia) in the developing brain (Hartfuss *et al.*, 2001). We cannot determine whether the increase that we observed in this marker was due to increased expression by individual cells or to an increased number of neural progenitor cells expressing *Glast-1*. We could not find any clue that astrocytes participate in the repair process in our model because the expression of *GFAP* and *S100β*, marker for astrocytes, is not elevated in our DNA microarray analysis and we could not detect any GFAP-positive astrocytes (Fig. 5). This is consistent with the fact that astrocytes are generated in the late stage of the embryonic period. On the other hand, astrocytes primarily mediate the repair of lesions in the adult brain with microglia (Fawcett & Asher, 1999; Silver & Miller, 2004). Glial scar and myelin-related proteins like Nogo are, however, known to inhibit the regeneration of injured adult brain. Taken together, this suggests that the embryonic brain might regenerate more easily because inhibitors, such as astrocytes or mature oligodendrocytes, are scant or absent in the prenatal stage.

We further identified up-regulated genes that are important for extracellular matrix, glycolysis and neural development. We believe that almost all of the up-regulated genes that we detected were induced in response to chemical-induced damage and in the subsequent recovery, and not via the DNA-demethylating effects of 5AzC. This is confirmed by the fact that genes whose expressions are known to be regulated by DNA methylation, such as *GFAP* and *S100β* (Takizawa *et al.*, 2001; Namihira *et al.*, 2004; Fan *et al.*, 2005), are not elevated in our model. This suggests that 5AzC exerts its damaging effect not by DNA demethylation but rather by DNA damage as discussed in our previous report (Ueno *et al.*, 2006).

The extracellular matrix is important in the remodeling that occurs after tissue damage. 5AzC treatment increased the gene expression of various types of collagen, laminin (1.32 ± 0.01 × increase at 24 h) and proteases (Table 1). Glycolysis is usually induced under hypoxic conditions. Chemical injury might induce hypoxia-like conditions, causing neural progenitor cells to up-regulate glycolytic genes. Hypoxia-inducible factors are the key transcription factors that respond to hypoxic conditions and control various target genes related to vascularization, glucose uptake/glycolysis, erythropoiesis, etc. (Bracken *et al.*, 2003; Michiels, 2004). We observed elevated

expression of two hypoxia-inducible factor targets, *P4ha1* and *Pkm2* (Fig. 6, Ca and Cb) (Bracken *et al.*, 2003). Further work is necessary to examine the expression of these transcription factors.

The expression of genes related to neural development is altered during the repair process, suggesting that tissue remodeling occurred. The normal, controlled expression patterns of these genes during brain development are critical for the formation of the complicated regional patterning of the brain (Rubenstein *et al.*, 1998; Grove & Fukuchi-Shimogori, 2003). We observed expression level changes in patterning-related genes that are expressed in a restricted region of the telencephalon, including *Fgf15* (Gimeno *et al.*, 2003), *Lhx5* (Sheng *et al.*, 1997), *Lhx2* (Monuki *et al.*, 2001), *Dlx5* (Eisenstat *et al.*, 1999) and *BF-1* (Dou *et al.*, 1999), although most genes are not shown in Table 1 because the fold change in expression is less than 1.5 (*Lhx5*, 1.42 ± 0.17 × increase at 36 h; *Lhx2*, −1.43 ± 0.04 × decrease at 24 h; *Dlx5*, −1.35 ± 0.03 × decrease at 24 h; *Bf-1*, −1.34 ± 0.03 × decrease at 24 h). It is unclear whether these changes in expression reflect changes in cell populations expressing the genes or if they reflect mechanisms controlling the proliferation, differentiation and patterning response to tissue damage. It would be interesting to examine how these types of genes affect the following brain patterning after prenatal injury. In addition, other genes are targets of the brain signaling molecules Wnt, Fgf and Shh, which play critical roles in the proliferation, differentiation and patterning of the developing brain (Altmann & Brivanlou, 2001; Salic *et al.*, 2005). For example, Lef1 (1.42 ± 0.06 × increase at 36 h) is a transcription factor in the Wnt signaling pathway (Galceran *et al.*, 2000). Fgfr3 is an Fgf receptor (Johnson & Williams, 1993; Bansal *et al.*, 2003) and the expression of Fgf15 is induced by Shh (Saitsu *et al.*, 2005). Some of these growth factors may influence the proliferation or differentiation of neural progenitor cells and help the regeneration. We therefore have to investigate the effect of these growth factors on the cell cycle kinetics in more detail (Caviness & Takahashi, 1995).

We show here that the developing brain has the capacity to respond to the damage induced by extrinsic chemical stresses, including changing the expression of numerous genes and recruiting microglia to aid the repair process. The degree of damage induced by extrinsic stresses, and the extent of the subsequent repair process, would dramatically influence the level of abnormalities that would appear in the neonatal brain. Our present results offer important insights into the mechanisms of repair and regeneration in the developing brain.

Acknowledgements

We thank Daniel Lee for his helpful comments on the manuscript. This study was supported financially by the Japan Society for the Promotion of Science.

Abbreviations

5AzC, 5-azacytidine; BS-I, lectin from *Bandeiraea simplicifolia*; CNS, central nervous system; DF, differentiating field; GAPDH, glyceraldehyde-3-phosphate dehydrogenase; GFAP, glial fibrillary acidic protein; IL, interleukin; M-CSF, macrophage colony stimulating factor; PCR, polymerase chain reaction; TNF, tumor necrosis factor; VZ, ventricular zone.

References

Alliot, F., Godin, I. & Pessac, B. (1999) Microglia derive from progenitors, originating from the yolk sac, and which proliferate in the brain. *Brain Res. Dev. Brain Res.*, **117**, 145–152.

Altmann, C. & Brivanlou, A. (2001) Neural patterning in the vertebrate embryo. *Int. Rev. Cytol.*, **203**, 447–482.

Ashwell, K. (1991) The distribution of microglia and cell death in the fetal rat forebrain. *Brain Res. Dev. Brain Res.*, **58**, 1–12.

Bansal, R., Lakhina, V., Remedios, R. & Tole, S. (2003) Expression of FGF receptors 1, 2, 3 in the embryonic and postnatal mouse brain compared with Pdgfralpha, Olig2 and Plp/dm20: implications for oligodendrocyte development. *Dev. Neurosci.*, **25**, 83–95.

Bracken, C.P., Whitelaw, M.L. & Peet, D.J. (2003) The hypoxia-inducible factors: key transcriptional regulators of hypoxic responses. *Cell. Mol. Life Sci.*, **60**, 1376–1393.

Burns, T.M., Clough, J.A., Klein, R.M., Wood, G.W. & Berman, N.E. (1993) Developmental regulation of cytokine expression in the mouse brain. *Growth Factors*, **9**, 253–258.

Calandra, T. & Roger, T. (2003) Macrophage migration inhibitory factor: a regulator of innate immunity. *Nat. Rev. Immunol.*, **3**, 791–800.

Caviness, V.S. & Takahashi, T. (1995) Proliferative events in the cerebral ventricular zone. *Brain Dev.*, **17**, 159–163.

Choi, B.H. (1989) The effects of methylmercury on the developing brain. *Prog. Neurobiol.*, **32**, 447–470.

Choi, J.S., Cha, J.H., Park, H.J., Chung, J.W., Chun, M.H. & Lee, M.Y. (2004) Transient expression of osteopontin mRNA and protein in amoeboid microglia in developing rat brain. *Exp. Brain Res.*, **154**, 275–280.

Costa, L.G., Aschner, M., Vitalone, A., Syversen, T. & Soldin, O.P. (2004) Developmental neuropathology of environmental agents. *Annu. Rev. Pharmacol. Toxicol.*, **44**, 87–110.

Cuadros, M.A. & Navascues, J. (1998) The origin and differentiation of microglial cells during development. *Prog. Neurobiol.*, **56**, 173–189.

Doetsch, F. (2003) The glial identity of neural stem cells. *Nat. Neurosci.*, **6**, 1127–1134.

Dou, C.L., Li, S. & Lai, E. (1999) Dual role of brain factor-1 in regulating growth and patterning of the cerebral hemispheres. *Cereb. Cortex*, **9**, 543–550.

Eisenstat, D.D., Liu, J.K., Mione, M., Zhong, W., Yu, G., Anderson, S.A., Ghattas, I., Puelles, L. & Rubenstein, J.L. (1999) *DLX-1, DLX-2*, and *DLX-5* expression define distinct stages of basal forebrain differentiation. *J. Comp. Neurol.*, **414**, 217–237.

Fan, G., Martinowich, K., Chin, M.H., He, F., Fouse, S.D., Hutnick, L., Hattori, D., Ge, W., Shen, Y., Wu, H., ten Hoeve, J., Shuai, K. & Sun, Y.E. (2005) DNA methylation controls the timing of astrogliogenesis through regulation of JAK-STAT signaling. *Development*, **132**, 3345–3356.

Fawcett, J.W. & Asher, R.A. (1999) The glial scar and central nervous system repair. *Brain Res. Bull.*, **49**, 377–391.

Galceran, J., Miyashita-Lin, E.M., Devaney, E., Rubenstein, J.L. & Grosschedl, R. (2000) Hippocampus development and generation of dentate gyrus granule cells is regulated by LEF1. *Development*, **127**, 469–482.

Gimeno, L., Brulet, P. & Martinez, S. (2003) Study of *Fgf15* gene expression in developing mouse brain. *Gene Expr. Patterns*, **3**, 473–481.

Grove, E.A. & Fukuchi-Shimogori, T. (2003) Generating the cerebral cortical area map. *Annu. Rev. Neurosci.*, **26**, 355–380.

Guerri, C. (2002) Mechanisms involved in central nervous system dysfunctions induced by prenatal ethanol exposure. *Neurotox. Res.*, **4**, 327–335.

Hanisch, U.K. (2002) Microglia as a source and target of cytokines. *Glia*, **40**, 140–155.

Hao, A.J., Dheen, S.T. & Ling, E.A. (2001a) Response of amoeboid microglia/brain macrophages in fetal rat brain exposed to a teratogen. *J. Neurosci. Res.*, **64**, 79–93.

Hao, A.J., Dheen, S.T. & Ling, E.A. (2001b) Induction of cytokine expression in the brain macrophages/amoeboid microglia of the fetal rat exposed to a teratogen. *Neuroreport*, **12**, 1391–1397.

Hao, A.J., Dheen, S.T. & Ling, E.A. (2002) Expression of macrophage colony-stimulating factor and its receptor in microglia activation is linked to teratogen-induced neuronal damage. *Neuroscience*, **112**, 889–900.

Hartfuss, E., Galli, R., Heins, N. & Gotz, M. (2001) Characterization of CNS precursor subtypes and radial glia. *Dev. Biol.*, **229**, 15–30.

Houle, J. & Das, G. (1983) Tissue repair in the embryonic rat spinal cord following exposure to N-ethyl-N-nitrosourea. *Int. J. Dev. Neurosci.*, **2**, 1–7.

Imai, Y. & Kohsaka, S. (2002) Intracellular signaling in M-CSF-induced microglia activation: role of Iba1. *Glia*, **40**, 164–174.

Johnson, D.E. & Williams, L.T. (1993) Structural and functional diversity in the FGF receptor multigene family. *Adv. Cancer Res.*, **60**, 1–41.

Katayama, K., Ishigami, N., Suzuki, M., Ohtsuka, R., Kiatipattanasakul, W., Nakayama, H. & Doi, K. (2000) Teratologic studies on rat perinates and offspring from dams treated with ethylnitrosourea (ENU). *Exp. Anim.*, **49**, 181–187.

Katayama, K., Ueno, M., Yamauchi, H., Nagata, T., Nakayama, H. & Doi, K. (2005a) Ethylnitrosourea induces neural progenitor cell apoptosis after

S-phase accumulation in a p53-dependent manner. *Neurobiol. Dis.*, **18**, 218–225.

Katayama, K., Ueno, M., Yamauchi, H., Nakayama, H. & Doi, K. (2005b) Microarray analysis of genes in fetal central nervous system after ethylnitrosourea administration. *Birth Defects Res. B Dev. Reprod. Toxicol.*, **74**, 255–260.

Kaur, C., Hao, A.J., Wu, C.H. & Ling, E.A. (2001) Origin of microglia. *Microsc. Res. Techn.*, **54**, 2–9.

Kikuchi-Horie, K., Kawakami, E., Kamata, M., Wada, M., Hu, J.G., Nakagawa, H., Ohara, K., Watabe, K. & Oyanagi, K. (2004) Distinctive expression of *midkine* in the repair period of rat brain during neurogenesis: immunohistochemical and immunoelectron microscopic observations. *J. Neurosci. Res.*, **75**, 678–687.

Kimler, B.F. (1998) Prenatal irradiation: a major concern for the developing brain. *Int. J. Radiat. Biol.*, **73**, 423–434.

Ling, E.A. & Wong, W.C. (1993) The origin and nature of ramified and amoeboid microglia: a historical review and current concepts. *Glia*, **7**, 9–18.

Lu, D.P., Nakayama, H., Shinozuka, J., Uetsuka, K., Taki, R. & Doi, K. (1998) 5-Azacytidine-induced apoptosis in the central nervous system of developing rat fetuses. *J. Tox. Path.*, **11**, 133–136.

Magavi, S.S., Leavitt, B.R. & Macklis, J.D. (2000) Induction of neurogenesis in the neocortex of adult mice. *Nature*, **405**, 951–955.

Mendola, P., Selevan, S.G., Gutter, S. & Rice, D. (2002) Environmental factors associated with a spectrum of neurodevelopmental deficits. *Ment. Retard. Dev. Disabil. Res. Rev.*, **8**, 188–197.

Michiels, C. (2004) Physiological and pathological responses to hypoxia. *Am. J. Pathol.*, **164**, 1875–1882.

Milligan, C.E., Cunningham, T.J. & Levitt, P. (1991) Differential immunohistochemical markers reveal the normal distribution of brain macrophages and microglia in the developing rat brain. *J. Comp. Neurol.*, **314**, 125–135.

Monuki, E.S., Porter, F.D. & Walsh, C.A. (2001) Patterning of the dorsal telencephalon and cerebral cortex by a roof plate–Lhx2 pathway. *Neuron*, **32**, 591–604.

Nakajima, K. & Kohsaka, S. (2001) Microglia: activation and their significance in the central nervous system. *J. Biochem.*, **130**, 169–175.

Namihira, M., Nakashima, K. & Taga, T. (2004) Developmental stage dependent regulation of DNA methylation and chromatin modification in an immature astrocyte specific gene promoter. *FEBS Lett.*, **572**, 184–188.

Oyanagi, K., Kakita, A., Yamada, M., Kawasaki, K., Hayashi, S. & Ikuta, F. (1998) Process of repair in the neuroepithelium of developing rat brain during neurogenesis: chronological and quantitative observation of DNA-replicating cells. *Brain Res. Dev. Brain Res.*, **108**, 229–238.

Picard-Riera, N., Nait-Oumesmar, B. & Baron-Van Evercooren, A. (2004) Endogeneous adult neural stem cells: limits and potential to repair the injured central nervous system. *J. Neurosci. Res.*, **76**, 223–231.

Rodier, P.M. (1995) Developing brain as a target of toxicity. *Environ. Health Perspect.*, **103**, 73–76.

Rubenstein, J.L., Shimamura, K., Martinez, S. & Puelles, L. (1998) Regionalization of the prosencephalic neural plate. *Annu. Rev. Neurosci.*, **21**, 445–477.

Saitsu, H., Komada, M., Suzuki, M., Nakayama, R., Motoyama, J., Shiota, K. & Ishibashi, M. (2005) Expression of the mouse *Fgf15* gene is directly initiated by Sonic hedgehog signaling in the diencephalon and midbrain. *Dev. Dyn.*, **232**, 282–292.

Salie, R., Niederkofler, V. & Arber, S. (2005) Patterning molecules: multitasking in the nervous system. *Neuron*, **45**, 189–192.

Sano, H., Hsu, D.K., Apgar, J.R., Yu, L., Sharma, B.B., Kuwabara, I., Izui, S. & Liu, F.T. (2003) Critical role of galectin-3 in phagocytosis by macrophages. *J. Clin. Invest.*, **112**, 389–397.

Sheng, H.Z., Bertuzzi, S., Chiang, C., Shawlot, W., Taira, M., Dawid, I. & Westphal, H. (1997) Expression of murine *Lhx5* suggests a role in specifying the forebrain. *Dev. Dyn.*, **208**, 266–277.

Shimada, M. & Langman, J. (1970) Repair of the external granular layer of the hamster cerebellum after prenatal and postnatal administration of methylazoxymethanol. *Teratology*, **3**, 119–133.

Silver, J. & Miller, H. (2004) Regeneration beyond the glial scar. *Nat. Rev. Neurosci.*, **5**, 146–156.

Sorokin, S.P., Hoyt, R.F. Jr, Blunt, D.G. & McNelly, N.A. (1992) Macrophage development. II. Early ontogeny of macrophage populations in brain, liver, and lungs of rat embryos as revealed by a lectin marker. *Anat. Rec.*, **232**, 527–550.

Sun, X., Inouye, M., Takagishi, Y., Hayasaka, S. & Yamamura, H. (1996) Follow-up study on histogenesis of microcephaly associated with ectopic gray matter induced by prenatal gamma-irradiation in the mouse. *J. Neuropathol. Exp. Neurol.*, **55**, 357–365.

Takizawa, T., Nakashima, K., Namihira, M., Ochiai, W., Uemura, A., Yanagisawa, M., Fujita, N., Nakao, M. & Taga, T. (2001) DNA methylation is a critical cell-intrinsic determinant of astrocyte differentiation in the fetal brain. *Dev. Cell*, **1**, 749–758.

Ueno, M., Katayama, K., Nakayama, H. & Doi, K. (2002a) Mechanisms of 5-azacytidine (5AzC)-induced toxicity in the rat foetal brain. *Int. J. Exp. Pathol.*, **83**, 139–150.

Ueno, M., Nakayama, H., Kajikawa, S., Katayama, K., Suzuki, K. & Doi, K. (2002b) Expression of ribosomal protein L4 (rpL4) during neurogenesis and 5-azacytidine (5AzC)-induced apoptotic process in the rat. *Histol. Histopathol.*, **17**, 789–798.

Ueno, M., Katayama, K., Yamauchi, H., Nakayama, H. & Doi, K. (2006) Cell cycle and cell death regulation of neural progenitor cells in the 5-azacytidine (5AzC)-treated developing fetal brain. *Exp. Neurol.*, **198**, 154–166.

Walther, M., Kuklinski, S., Pesheva, P., Guntinas-Lichius, O., Angelov, D.N., Neiss, W.F., Asou, H. & Probstmeier, R. (2000) *Galectin-3* is upregulated in microglial cells in response to ischemic brain lesions, but not to facial nerve axotomy. *J. Neurosci. Res.*, **61**, 430–435.

Zhou, Q., Wang, S. & Anderson, D.J. (2000) Identification of a novel family of oligodendrocyte lineage-specific basic helix-loop-helix transcription factors. *Neuron*, **25**, 331–343.

Available online at www.sciencedirect.com
SCIENCE DIRECT®
Experimental and Molecular Pathology 79 (2005) 224 – 228
Experimental and Molecular Pathology
www.elsevier.com/locate/yexmp

Changes in cytochrome P450 isozymes (CYPs) protein levels during lactation in rat liver

Xi Jun He, Noriko Ejiri, Hiroyuki Nakayama, Kunio Doi *

Department of Veterinary Pathology, Graduate School of Agricultural and Life Sciences, The University of Tokyo, 1-1-1 Yayoi, Bunkyo-ku, Tokyo 113-8657, Japan

Received 16 August 2005
Available online 14 October 2005

Abstract

The effects of pregnancy on CYPs protein level in the liver have been investigated in our previous study. Since pregnancy was associated with a decrease in CYPs protein level, the objective of this study was to investigate whether CYPs protein can revert to the virgin control level after delivery. Western blot analysis was performed to investigate the changes of total nine CYPs protein (CYP1A1, CYP2B1/CYP2B2, CYP2C6, CYP2C12, CYP2D1, CYP2D4, CYP2E1, CYP3A1 and CYP4A1) at three distinct phases: delivery (postpartum day 0, PPD 0), peak lactation (PPD 14) and on weaning (PPD 28). By PPD 0, CYP1A1, 2B1, 2B2, 2C6, 2E1 and CYP4A1 were markedly down-regulated when compared with virgin controls. By PPD 14, however, CYP1A1, 2B1, 2B2 and CYP2C6 returned to the virgin control level. All the decreased CYPs during lactation were at the virgin control level at PPD 28. The expression of CYP2C12, CYP2D1 and CYP 3A1 did not differ between lactating, post-lactation and virgin control rats. CYP2D4 was not detectable in microsomal proteins obtained from virgin control rats at a protein loading of 20 μg total protein per lane.

Keywords: CYPs; F344 rat; Western blot analysis; Lactation

Introduction

The cytochrome P450 (CYP) enzyme system is extremely important for the metabolism of xenobiotics as well as endogenous substances, such as fatty acids, prostaglandins and steroids (Lind et al., 2003). Expression of CYP isozymes (CYPs) is also known to be influenced by a variety of endogenous and foreign factors such as inflammation, age, gender, nutritional status, pregnancy and so on. Pregnancy is a physiological state accompanied by a high metabolic demand and an increased requirement for tissue oxygen (Spatling et al., 1992). A body of evidence suggests that pregnancy may be responsible for the depression in the microsomal enzyme activity and the reduction in the total content of CYP in the rat liver (Feuer and Liscio, 1969; Guarino et al., 1969; Neale and Parke, 1973; Dean and Stock, 1975, 1989). We have previously demonstrated that pregnancy is associated with decreased hepatic levels of some CYPs proteins in midpregnancy and/or late pregnancy (He et al., 2005). It has been suggested that changes in the physiological state of an animal may alter CYPs ability to metabolize foreign chemicals (Borlakoglu et al., 1993). The hormonal changes that occur during pregnancy and at the start of lactation are complex, and the balance between the various hormones during lactation is different from that during pregnancy and different again from that in the virgin animal (Smith, 1975). In the lactating animals, milk production introduces an additional metabolic system which competes for the available nutrients with other processes such as the formation of body reserves.

A few studies have been performed on the effects of lactation on tissue metabolism and activities of some enzymes. Smith (1975) has demonstrated that the activities of some enzymes in the rat liver could be influenced by pregnancy and lactation. Based on their observations, Abel et al. (1979) have suggested that drug disposition may be altered during lactation. Review by Williamson (1986) suggests that the main aim of changes in tissue metabolism during rat lactation is to preserve the increased intake of nutrients from diet for milk production. Smith et al. (1998) have demonstrated that major changes in hepatic lipid metabolism must occur to maintain cholesterol homeostasis during rat lactation.

* Corresponding author. Fax: +81 3 5841 8185.
E-mail address: akunio@mail.ecc.u-tokyo.ac.jp (K. Doi).

0014-4800/$ - see front matter © 2005 Elsevier Inc. All rights reserved.
doi:10.1016/j.yexmp.2005.08.009

Table 1
Body and liver weights

Postpartum day (PPD)	Body weight	Liver weight
Virgin control	143.70 ± 1.66	5.78 ± 0.34
PPD 0	156.70 ± 6.61*	7.38 ± 1.17
PPD 14	184.50 ± 5.91***	8.23 ± 0.40**
PPD 28	188.03 ± 17.39*	7.60 ± 1.13

Data are represented as mean ± SD of 6 rats. *$P < 0.05$, **$P < 0.01$, ***$P < 0.001$; significantly different from virgin controls.

It is assumed that, therefore, lactation may also be involved in the regulation of hepatic CYPs expression like pregnancy. Borlakoglu et al. (1993) investigated the alterations of some CYPs in the rat liver during lactation. Western immunoblot analysis of microsomal proteins obtained from pregnant and lactating rats showed that only CYP2C6 and CYP3A1 proteins are expressed at detectable levels, while the expression of others was not detectable in pregnant and lactating rats at a protein loading of 3 μg total protein per well. In their study, comparison was not performed between lactating and virgin control rats. During the past few decades, much less attention has been given to the effect of lactation on the regulation of hepatic CYPs expression. It was therefore of interest to investigate the effect of lactation on the expression of hepatic CYPs proteins. Attention is also paid to some CYPs, which were down-regulated during pregnancy in our previous study, whether and when they could return to the control virgin level. For this purpose, changes in protein levels of nine CYPs in the lactating and post-lactation rat liver were investigated by Western blot analysis at three distinct phases: delivery (postpartum day 0, PPD 0), peak lactation (PPD 14) and on weaning (PPD 28).

Materials and methods

Animals

Twelve pregnant and six age-matched virgin control rats (11 weeks of age) were purchased from Saitama Experimental Animal Co. (Saitama, Japan) and used in this study. The day of delivery recognized was designated as postpartum day 0 (PPD 0). The rats were individually housed in plastic cages in an animal room controlled at 23 ± 2°C and at 55 ± 5% humidity condition with 14 h/10 h light/dark cycle and fed pellets (MF, Oriental Yeast Co., Ltd.,

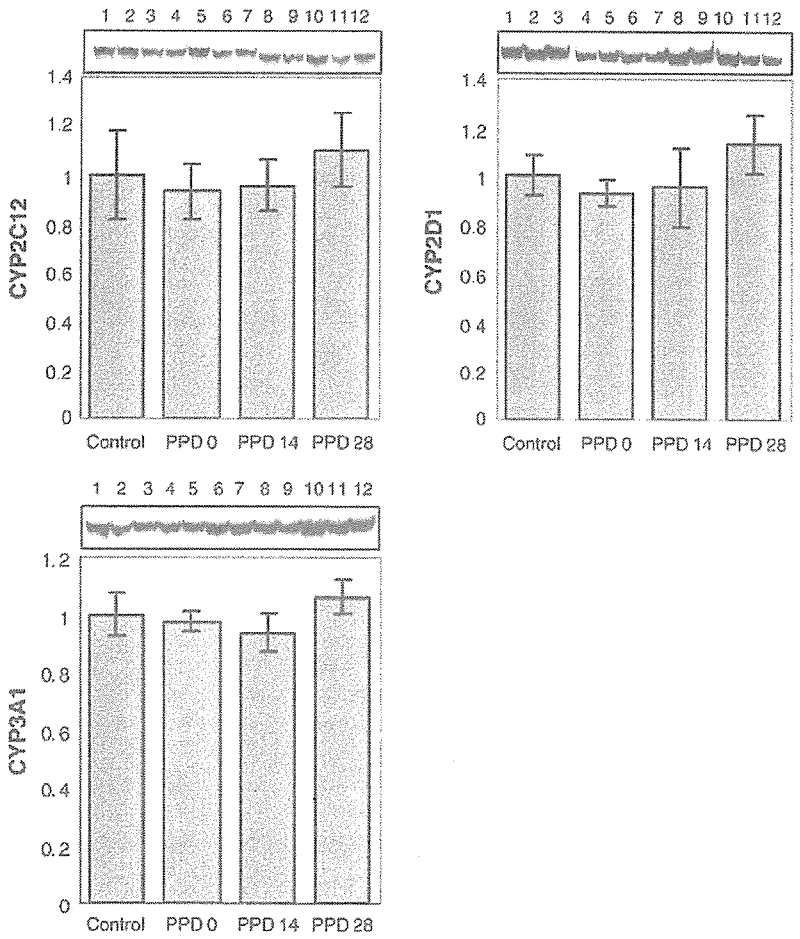

Fig. 1. Western blot analysis of liver microsomes from virgin control, lactating (PPD 0, PPD 14) and post-lactation (PPD 28) rats. The amount of protein per lane was 20 μg (CYP2C12, CYP2D1 and CYP3A1). Lanes 1 to 3: age-matched virgin control rats; lanes 4 to 6: PPD 0 rats; lanes 7 to 9: PPD 14 rats; lanes 10 to 12: PPD 28 rats. Densitometry of Western blotting using monoclonal antibodies against rat hepatic CYP2C12, CYP2D1 and CYP3A1 was performed. Values are expressed as the ratio of lactation (PPD 0 and PPD 14) and post-lactation (PPD 28)/virgin control in arbitrary densitometric units of protein amounts and reported as the means ± SD of 6 rats.

Tokyo, Japan) and water ad libitum. On PPD 0, PPD 14 (peak lactation) and PPD 28 (7 days post-lactation), 6 dams were sacrificed under ether anesthesia, respectively. Livers were removed and used for Western blot analysis. Age-matched virgin rats were used as controls.

Western blot analysis

Livers were homogenized in ice-cold 0.1 M phosphate buffer (PB), pH 7.4, containing 150 mM KCl, 1 mM EDTA Na, 1 mM DTT and microsomes were prepared by differential centrifugation. Briefly, the liver homogenates were centrifuged at 9000 × *g* for 20 min at 4°C, and the resulting supernatant was centrifuged at 105,000 × *g* for 1 h at 4°C. After discarding the supernatant, the pellets were suspended in the same buffer and re-centrifuged. The pellets were re-suspended with 0.1 M PB, pH 7.4, containing 150 mM KCl, 20% glycerol, 1 mM EDTA Na, 1 mM DTT, and stored at −80°C until used. Protein concentration of the samples was measured using bovine serum albumin (BSA) as the standard. Microsomal proteins (20 or 40 μl) were separated using SDS-PAGE in 10% polyacrylamide gels and electrophoretically transferred to polyvinylidene difluoride (PVDF) membrane (Bio-Rad, Richmond, CA), and the plate was blocked with 8% skim milk/TBS for 1 h at room temperature. The membrane was then incubated with the abovementioned anti-rat CYP1A1, CYP2B1/2B2, CYP2C6, CYP2C12, CYP2D1, CYP2D4, CYP2E1, CYP3A1 and CYP4A1 antibodies diluted in 8% skim milk/TBS (1:200) overnight at 4°C followed by another 1 h incubation with horseradish-peroxidase-conjugated secondary antibodies (donkey anti-rabbit IgG; Amersham Pharmacia Biotech Ltd., Arlington Heights IL) and rabbit anti-goat IgG (Cappel, Aurora, OH)). The protein bands were visualized by ECL plus Western blotting detection system (Amersham Pharmacia Biotech Ltd., Arlington Heights, IL) followed by a brief exposure to Hyperfilm (Amersham Biosciences UK Ltd.). Quantity One v3.0 software (PDI, Inc, NY, USA) was used to quantitate the band intensities.

Statistical analysis

Results were presented as the mean ± standard deviation (SD) of six rats. Student's *t* test was employed to calculate the statistical significance between virgin control and postpartum (PPD 0, PPD 14 and PPD 28) groups.

Results

Change in body and liver weights

There were significant increases in the body weights on PPD 0, PPD 14 and PPD 28 compared with virgin controls.

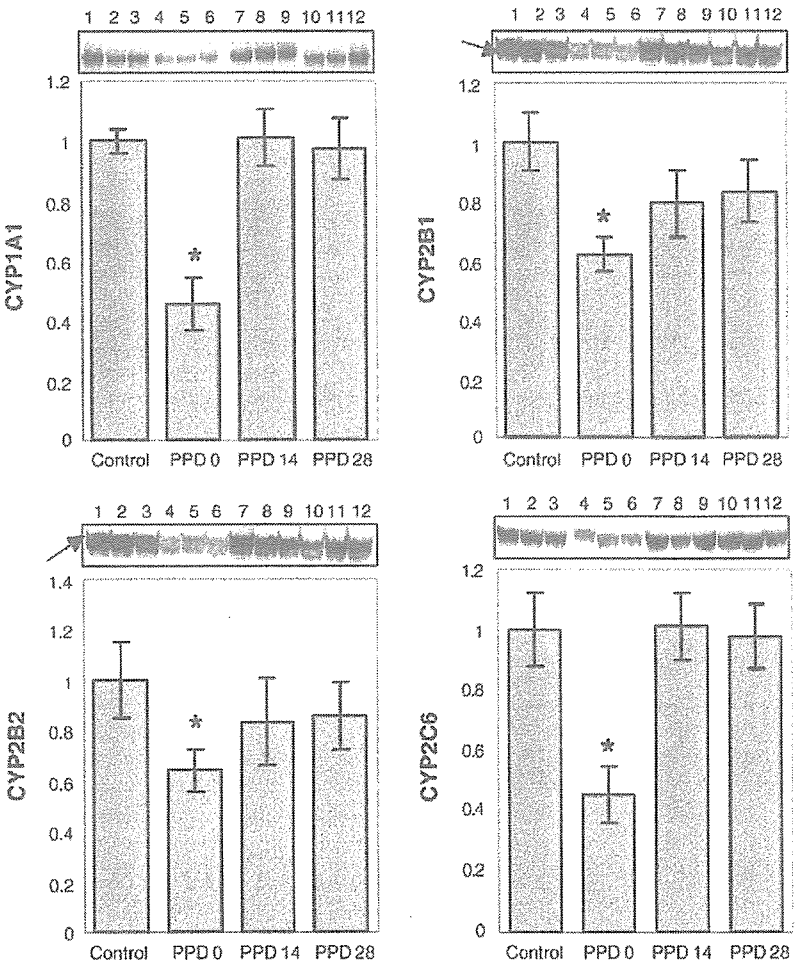

Fig. 2. Western blot analysis of liver microsomes from virgin control, lactating (PPD 0, PPD 14) and post-lactation (PPD 28) rats. The amount of protein per lane was 20 μg (CYP2B1/2 and CYP2C6) and 40 μg (CYP1A1). Lanes 1 to 3: age-matched virgin control rats; lanes 4 to 6: PPD 0 rats; lanes 7 to 9: PPD 14 rats; lanes 10 to 12: PPD 28 rats. Densitometry of Western blotting using monoclonal antibodies against rat hepatic CYP1A1, CYP2B1/2 and CYP2C6 was performed. Values are expressed as the ratio of lactation (PPD 0 and PPD 14) and post-lactation (PPD 28)/virgin control in arbitrary densitometric units of protein amounts and reported as the means ± SD of 6 rats. * Significantly different from virgin controls at $P < 0.05$.

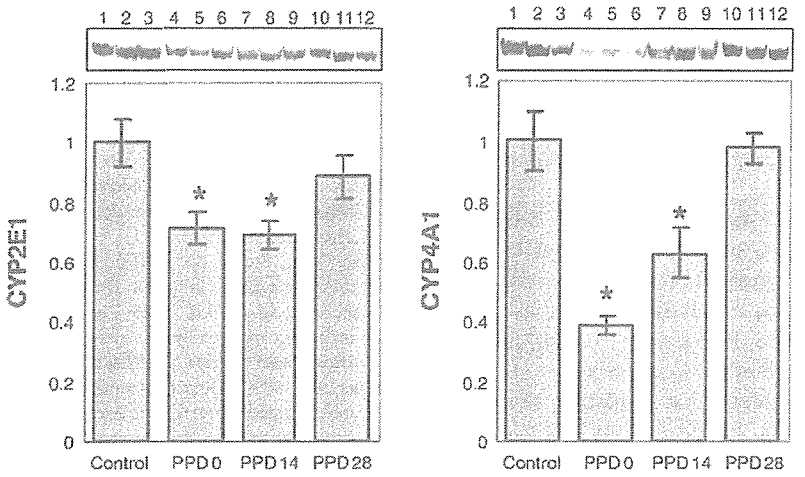

Fig. 3. Western blot analysis of liver microsomes from virgin control, lactating (PPD 0, PPD 14) and post-lactation (PPD 28) rats. The amount of protein per lane was 20 μg (CYP2E1) and 40 μg (CYP4A1). Lanes 1 to 3: age-matched virgin control rats; lanes 4 to 6: PPD 0 rats; lanes 7 to 9: PPD 14 rats; lanes 10 to 12: PPD 28 rats. Densitometry of Western blotting using monoclonal antibodies against rat hepatic CYP2E1 and CYP4A1 was performed. Values are expressed as the ratio of lactation (PPD 0 and PPD 14) and post-lactation (PPD 28)/virgin control in arbitrary densitometric units of protein amounts and reported as the means ± SD of 6 rats. * Significantly different from virgin controls at $P < 0.05$.

However, the increase in body weight was not accompanied with the increase in liver weight when detected on PPD 0 and PPD 28 (Table 1). On PPD 14, there was a significant increase in the liver weight compared with virgin controls (Table 1).

Findings of Western blot analysis

The results of Western blot analysis are shown in Figs. 1–3. The expression of CYP2C12, CYP2D1 and CYP 3A1 proteins did not differ between age-matched virgin control and experimental rats (at PPD 0, PPD 14 and PPD 28) (Fig. 1). CYP2D4 was not detectable in microsomal proteins obtained from virgin controls and experimental animals at a protein loading of 20 μg total protein per lane. Fig. 2 shows significant decreases in the CYP1A1, CYP2B1, CYP2B2 and CYP2C6 contents when detected on postpartum day 0 (45.3%, 61.9%, 63.8% and 45.3% of age-matched virgin control values, respectively). They returned to the virgin control levels by PPD 14 and kept constant levels on PPD 28 (Fig. 2). Decreases in CYP2E1 and CYP4A1 protein levels (71.3% and 39.0% of age-matched virgin control levels) were also found on PPD 0 (Fig. 3), and they were still decreased on PPD 14 (69.3% and 62.3% of virgin control levels). By PPD 28, CYP2E1 and CYP4A1 protein levels returned to virgin control levels.

Discussion

In the present study, in comparison with age-matched virgin control rats, lactating rats showed significantly decreased hepatic levels of six out of nine CYPs proteins (CYP1A1, CYP2B1, CYP2B2, CYP2C6, CYP2E1 and CYP4A1) at day of delivery (PPD 0). By PPD 21 (peak lactation), CYP1A1, CYP2B1, CYP2B2 and CYP2C6 proteins returned to the virgin control levels. All of the hepatic CYPs proteins were at virgin control level at 7 days post-lactation (PPD 28).

We previously demonstrated that pregnancy is associated with decreased hepatic levels of three (CYP2B2, CYP2C6 and CYP4A1) and six CYPs proteins (CYP1A1, CYP2B1, CYP2B2, CYP2C6, CYP2E1 and CYP4A1) in midpregnancy and late pregnancy, respectively. Based on the marked decreases in the same six CYPs proteins at PPD 0, it is obvious that they kept decreased protein levels even though the physiological state has been changes.

In the present study, peak lactation (PPD 14) was linked to an increase in liver weight by up to 42.4%. Although it has been suggested that a decrease in mixed-function oxidase activity during pregnancy is due to a reduction in the hepatocellular capacity to metabolize drugs with an increase in liver size (Symons et al., 1982), it could not be used, however, for interpreting during lactation. Since six CYPs proteins were decreased on PPD 0, not accompanying with an increase in liver weight. Of six decreased CYPs proteins, four returned to the virgin control levels on PPD 14. Based on these observations, it is clear that liver enlargement is not involved in the decrease in CYPs protein during rat lactation.

Progesterone and its metabolites have been suggested to be involved in regulation of activities of the hepatic drug metabolizing enzymes during pregnancy (Feuer, 1979). However, once lactation begins, prolactin is increased, and progesterone is decreased and disappears immediately. Prolactin is essential not only for the initiation of lactation after parturition but also for the maintenance of lactation. In addition to prolactin, successful lactation also requires the hormone oxytocin (Heil and Subramanian, 1998). Dean and Stock (1975) have suggested that lower levels of hepatic microsomal enzyme activity might reflect a biological control mechanism to ensure the elevated levels of progesterone required to maintain the pregnant state. Similarly, down-regulation of CYPs protein probably occurs in response to the hormonal demand for milk production during lactation. In the present study, six out of nine CYPs were down-regulated at

PPD 0 and returned to the virgin control level at PPD 28 (on weaning), indicating that this biological control mechanism may also be present during lactation. Experiments remain to be performed on whether prolactin and/or oxytocin could suppress the activities of drug metabolizing enzymes and reduce CYPs protein.

Oxidative stress may be one of the factors which are responsible for the regulation of CYPs during rat lactation. Oxidative stress has been suggested to result in the reduction of total CYP450 levels and drug metabolizing activities in vivo (Mannering and Deloria, 1986; Peristeris et al., 1992; Gatti et al., 1993; Liu et al., 1993). Furthermore, Barker et al. (1994) have investigated the possibility that oxidative stress may influence inducer-dependent expression of CYP1A1 and CYP1A2 and demonstrated that hydrogen peroxide suppresses the accumulation of CYP1A1 and CYP1A2 mRNAs in isolated hepatocytes through a transcriptional mechanism. Pahan et al. (1997) demonstrated that there is a down-regulation of CYP2E1 in rat liver peroxisomes by a mechanism of ischemia/reperfusion-induced oxidative stress. Investigation by Upreti et al. (2002) indicated that significantly higher lipid peroxidation levels were established in all the major organs of rat during lactation. Furthermore, they also demonstrated that the early lactation generated higher oxidative stress compared with the late periods of lactation. This seems to be consistent with our data: six CYPs proteins were markedly decreased at PPD 0, and four of them returned to the virgin control level on PPD 14. In human, lipid peroxidation is increased during pregnancy, and delivery alone is a major source of oxidative stress (Arikan et al., 2001), probably confirming the results obtained at PPD 0 in this study. Therefore, oxidative stress may play a role in the regulation of CYPs protein during rat lactation.

Although endogenous nitric oxide (NO), a potent vasodilator and a platelet anti-aggregating factor, has been suggested to be involved in the regulation of CYPs protein during rat pregnancy (He et al., 2005), the data of changes in NO during rat lactation are absent.

Taken together, the results of the present study suggest that rat lactation is accompanied with decreases in some CYPs proteins levels. Effects of lactation on decreases in CYPs protein levels were more predominant at birth day (PPD 0) than at peak lactation (PPD 14). All the decreased CYPs proteins were at virgin control levels by 7 days post-lactation (PPD 28), clearly suggesting that biological changes during rat lactation could influence the expression of hepatic CYPs protein. Further studies are required to elucidate the mechanism of effects of lactation on down-regulation of CYPs protein.

References

Abel, E.L., Greizerstein, H.B., Siemens, A.J., 1979. Influence of lactation on rate of disappearance of ethanol in the rat. Neurobehav. Toxicol. 1, 185–186.

Arikan, S., Konukoglu, D., Arikan, C., Akcay, T., Davas, I., 2001. Lipid peroxidation and antioxidant status in maternal and cord blood. Gynecol. Obstet. Invest. 51, 145–149.

Barker, C.W., Fagan, J.B., Pasco, D.S., 1994. Down-regulation of P4501A1 and P4501A2 mRNA expression in isolated hepatocytes by oxidative stress. J. Biol. Chem. 269, 3985–3990.

Borlakoglu, J.T., Scott, A., Henderson, C.J., Wolf, C.R., 1993. Alterations in rat hepatic drug metabolism during pregnancy and lactation. Biochem. Pharmacol. 46, 29–36.

Dean, M.E., Stock, B.H., 1975. Hepatic microsomal metabolism of drugs during pregnancy in the rat. Drug Metab. Dispos. 3, 325–331.

Dean, M.E., Stock, B.H., 1989. The influence of phenobarbital administration on hepatic monooxygenase activity at various stages of gestation in the rat. Drug Metab. Dispos. 17, 579–581.

Feuer, G., 1979. Action of pregnancy and various progesterones on hepatic microsomal activities. Drug Metab. Rev. 9, 147–169.

Feuer, G., Liscio, A., 1969. Origin of delayed development of drug metabolism in the newborn rat. Nature 223, 68–70.

Gatti, S., Faggioni, R., Echtenacher, B., Ghezzi, P., 1993. Role of tumour necrosis factor and reactive oxygen intermediates in lipopolysaccharide-induced pulmonary oedema and lethality. Clin. Exp. Immunol. 91, 456–461.

Guarino, A.M., Gram, T.E., Schroeder, D.H., Call, J.B., Gillette, J.R., 1969. Alterations in kinetic constants for hepatic microsomal aniline hydroxylase and ethylmorphine *N*-demethylase associated with pregnancy in rats. J. Pharmacol. Exp. Ther. 168, 224–228.

He, X.J., Ejiri, N., Nakayama, H., Doi, K., 2005. Effects of pregnancy on CYPs protein expression in rat liver. Exp. Mol. Pathol. 78, 64–70.

Heil, S.H., Subramanian, M.G., 1998. Alcohol and the hormonal control of lactation. Alcohol Health Res. World 22, 178–184.

Lind, A.B., Wadelius, M., Darj, E., Finnstrom, N., Lundgren, S., Rane, A., 2003. Gene expression of cytochrome P450 1B1 and 2D6 in leukocytes in human pregnancy. Pharmacol. Toxicol. 92, 295–299.

Liu, P.T., Kentish, P.A., Symons, A.M., Parke, D.V., 1993. The effects of ether anaesthesia on oxidative stress in rats-dose response. Toxicology 80, 37–49.

Mannering, G.J., Deloria, L.B., 1986. The pharmacology and toxicology of the interferons: an overview. Annu. Rev. Pharmacol. Toxicol. 26, 455–515.

Neale, M.G., Parke, D.V., 1973. Effects of pregnancy on the metabolism of drugs in the rat and rabbit. Biochem. Pharmacol. 22, 1451–1461.

Pahan, K., Smith, B.T., Singh, A.K., Singh, I., 1997. Cytochrome P-450 2E1 in rat liver peroxisomes: downregulation by ischemia/reperfusion-induced oxidative stress. Free Radical Biol. Med. 23, 963–971.

Peristeris, P., Clark, B.D., Gatti, S., Faggioni, R., Mantovani, A., Mengozzi, M., Orencole, S.F., Sironi, M., Ghezzi, P., 1992. *N*-acetylcysteine and glutathione as inhibitors of tumor necrosis factor production. Cell. Immunol. 140, 390–399.

Smith, R.W., 1975. The effects of pregnancy and lactation on the activities in rat liver of some enzymes associated with glucose metabolism. Biochim. Biophys. Acta 411, 22–29.

Smith, J.L., Lear, S.R., Forte, T.M., Ko, W., Massimi, M., Erickson, S.K., 1998. Effect of pregnancy and lactation on lipoprotein and cholesterol metabolism in the rat. J. Lipid Res. 39, 2237–2249.

Spatling, L., Fallenstein, F., Huch, A., Huch, R., Rooth, G., 1992. The variability of cardiopulmonary adaptation to pregnancy at rest and during exercise. Br. J. Obstet. Gynaecol. 99, 1–40.

Symons, A.M., Turcan, R.G., Parke, D.V., 1982. Hepatic microsomal drug metabolism in the pregnant rat. Xenobiotica 12, 365–374.

Upreti, K., Chaki, S.P., Misro, M.M., 2002. Evaluation of peroxidative stress and enzymatic antioxidant activity during pregnancy and lactation in rats. Health Popul., Perspect. Issues 25, 177–185.

Williamson, D.H., 1986. Regulation of metabolism during lactation in the rat. Reprod. Nutr. Dev. 26, 597–603.

J Toxicol Pathol 2006; 19: 15–27

Review

T-2 Toxin and Apoptosis

Kunio Doi[1], Junko Shinozuka[2], and Shinya Sehata[3]

[1]Department of Veterinary Pathology, Graduate School of Agricultural and Life Sciences, The University of Tokyo, 1–1–1 Yayoi, Bunkyo, Tokyo 113–8657, Japan
[2]Exploratory Toxicology and DMPK Research Laboratories, Tanabe Seiyaku Co., Ltd., 2–50 Kawagishi, Toda-shi, Saitama 335–8505, Japan
[3]Medical Safety Research Laboratories, Sankyo Co., Ltd., 717 Horikoshi, Fukuroi-shi, Shizuoka 437–0065, Japan

Abstract: T-2 toxin is a cytotoxic fungal secondary metabolite produced by various species of *Fusarium*. This paper reviews the reported data about the development and/or mechanisms of T-2 toxin-induced apoptosis in the hematopoietic, lymphoid and gastrointestinal tissues, dorsal skin and fetal tissues of mice and rats. Apoptosis occurs earlier in hematopoietic tissues than in lymphoid tissues, and moreover there is a difference among lymphocyte populations in the susceptibility to T-2 toxin. *C-fos* plays an important role in the early phase of T-2 toxin-induced apoptosis in hematopoietic and lymphoid tissues through mobilization of $[Ca^{2+}]_i$ and the PKC-dependent pathway, but not through Fas/Fasligand or p53-related pathways. In the gastrointestinal tract, apoptosis develops earlier in the small intestine than in the stomach, and is more prominent in the small intestine than in the large intestine. In the dorsal skin topically treated with T-2 toxin, epidermal basal cell proliferating activity is first suppressed due to the elevated TGF-β_1 expression, and then basal cell apoptosis develops concomitantly with the elevation of *c-fos*, *c-jun* and *TNF-*α mRNAs expression. In the fetuses, T-2 toxin-induced apoptosis is mainly observed in the central nervous and skeletal systems. In the fetal brain, T-2 toxin induces oxidative stress, followed by activation of the MAPK-JNK-c-Jun pathway, finally resulting in apoptosis. The TNF receptor pathway may also be involved in T-2 toxin-induced apoptosis in the fetal brain. Thus, the development and mechanisms of T-2 toxin-induced apoptosis differ somewhat depending on the tissues affected. (J Toxicol Pathol 2006; **19**: 15–27)

Key words: T-2 toxin, apoptosis, development, mechanisms, rat, mice

Introduction

T-2 toxin is a cytotoxic fungal secondary metabolite, produced by various species of *Fusarium* (*F. sporotichioides*, *F. poae*, *F. equiseti*, *F. acuminatum*), which infect corn, wheat, barley and rice crops in the field or during storage[1,2]. T-2 toxin is a member of a large group of sesquiterpenoid fungal metabolites, called trichothecenes, which have a common skeleton that includes a double bond between C9 and 10 and an epoxide group at C12 and 13[3]. Up to the present, 148 naturally occurring trichothecenes have been isolated, and they are classified into four types: A-D. T-2 toxin belongs to type A trichothecenes and its chemical structure was elucidated in 1986 by Bamberg *et al.*[4] (Fig. 1). The natural occurrence of T-2 toxin in raw agricultural commodities has been recorded in many countries (Finland, 1979; Hungary, 1983; Taiwan, 1983; India, 1987, 1989; Egypt, 1987, New Zealand, 1989; Canada, 1979–82; Poland, 1997; Denmark, 1998–2000), and T-2 toxin intoxication is still a serious problem.

Fusarium spp. affects human and farm animals by producing either mycotoxicosis or invasive diseases. A disease known as "alimentary toxic aleukia (ATA)", characterized by leukopenia, agranulocytosis, hemorrhagic diathesis, bone marrow aplasia and sepsis, caused the death of hundreds of thousands of people in the USSR during the World War II[5]. The disease occurred after the ingestion of overwintered cereal grains colonized with *F.*

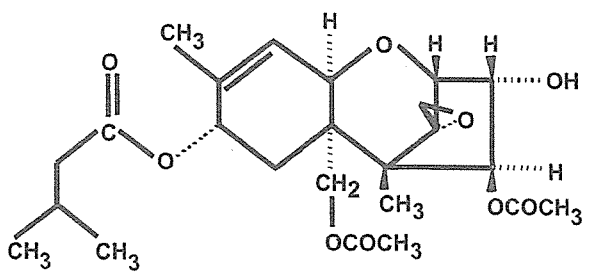

Fig. 1. Chemical structure of T-2 toxin.

Received: 11 February 2006, Accepted: 14 February 2006
Mailing address: Kunio Doi, Department of Veterinary Pathology, Graduate School of Agricultural and Life Sciences, The University of Tokyo, 1–1–1 Yayoi, Bunkyo, Tokyo 113–8657, Japan
TEL: 81-3-5841-5400 FAX: 81-3-5841-8185
E-mail: akunio@mail.ecc.u-tokyo.ac.jp

sporotrichioides and *F. poae*, high producers of T-2 toxin[6]. In Japan, outbreaks of a similar disease called "Akakabi-byo" in human and farm animals and hemorrhagic syndrome in horses ("bean-hull poisoning of horses") have been associated with grains contaminated with T-2 toxin and other trichothecenes[2,7].

The toxic effects of T-2 toxin have been studied in many animal species such as experimental animals, chickens, ducks, cattle, sheep and pigs. All animal species tested were sensitive to this mycotoxin. Pigs are the most sensitive among farm animals[8], and rats are more sensitive than mice. Oral, parenteral and cutaneous exposure to trichothecene mycotoxins produces lesions in hematopoietic, lymphoid and gastrointestinal tissues and functional suppression of reproductive organs[9–12]. Cardiomyopathy has been reported after topical application of T-2 toxin to rats[13], and signs somewhat similar to those in human ATA have been reported in rhesus monkeys and cats fed T-2 toxin[14].

The toxicokinetics of T-2 toxin have been studied using various animal species. One or more biotransformations, i.e. deacylation, hydroxylation, glucuronide conjugation, deacetylation and de-epoxidation occur during the metabolism of T-2 toxin by different systems[3]. The plasma radioactivity reaches a peak at 30 min after oral administration of ^{3}H-T-2 toxin to mice, and T-2 toxin is rapidly metabolized in the liver and other tissues and eliminated into the feces and urine[15]. The plasma elimination half-time of T-2 toxin and its metabolites in pigs is approximately 90 min[16]. After intra-aortal administration in pigs, the tissue concentrations of T-2 toxin are consistently highest in lymphoid organs, and detectable amounts are present in the spleen and mesenteric lymph nodes at 3 hours after administration[17]. Enterohepatic circulation of T-2 toxin and its metabolites through glucuronide conjugation has been reported in rats[18].

T-2 toxin is a well-known inhibitor of protein synthesis through its high binding affinity to the peptidyltransferase which is an integral part of the 60s ribosomal subunit[8,19,20]. T-2 toxin also inhibits the synthesis of DNA and RNA, probably secondarily to the inhibition of protein synthesis[8,21]. Moreover, T-2 toxin interferes with the metabolism of membrane phospholipids and increases liver lipid peroxides[22,23]. However, the exact mechanism of T-2 toxin-induced cell death has remained unclear for many years. In this regard, Quiroga *et al.*[24] reported the ultrastructural changes of thymocytes suggesting the occurrence of apoptosis in T-2 toxin-inoculated mice (Fig. 2). Later, Shinozuka *et al.*[25] clarified from multiple viewpoints that T-2 toxin-induced lymphoid cell death is apoptosis. This is the first report of mycotoxin-induced apoptosis. Now, it is known that T-2 toxin is able to induce apoptosis in many types of cells with high proliferating activity (Fig. 3). Apoptosis is usually confirmed by histology (pyknosis or karyorrhexis), *in situ* detection of fragmented DNA (TUNEL method)[26], ultrastructure (shrinkage of the cell body and condensation of nuclear chromatin, and apoptotic body formation) and DNA agarose gel electrophoresis (ladder formation). Flow cytometry is also used to detect early-phase apoptosis.

Fig. 2. Apoptotic thymocyte (arrow) and apoptotic body ingested by epithelial cell (b).

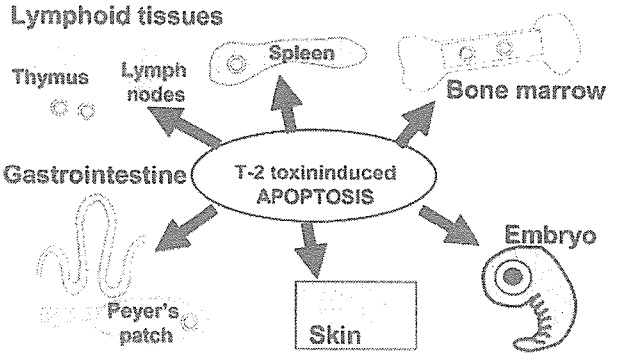

Fig. 3. Target organs of T-2 toxin-induced apoptosis.

This article reviews the data reported about the development and/or mechanisms of T-2 toxin-induced apoptosis in hematopietic, lymphoid and gastrointestinal tissues, dorsal skin, and fetal tissues of mice and rats.

Hematopoietic Tissues

In mice orally treated with T-2 toxin, the bone marrow shows a significant hypocellularity. The number of myelocytes significantly decreases due to the loss of immature granulocytes, erythroblasts and lymphocytes by apoptosis, and granulocytes and erythroblasts decrease earlier than lymphocytes (Fig. 4). On the other hand, mature granulocytes show no significant changes[27]. Such changes in the hematopoietic tissues result in a significant depression in the number of white blood cells in peripheral blood[27–29].

The spleen, which is composed of white and red pulp, is

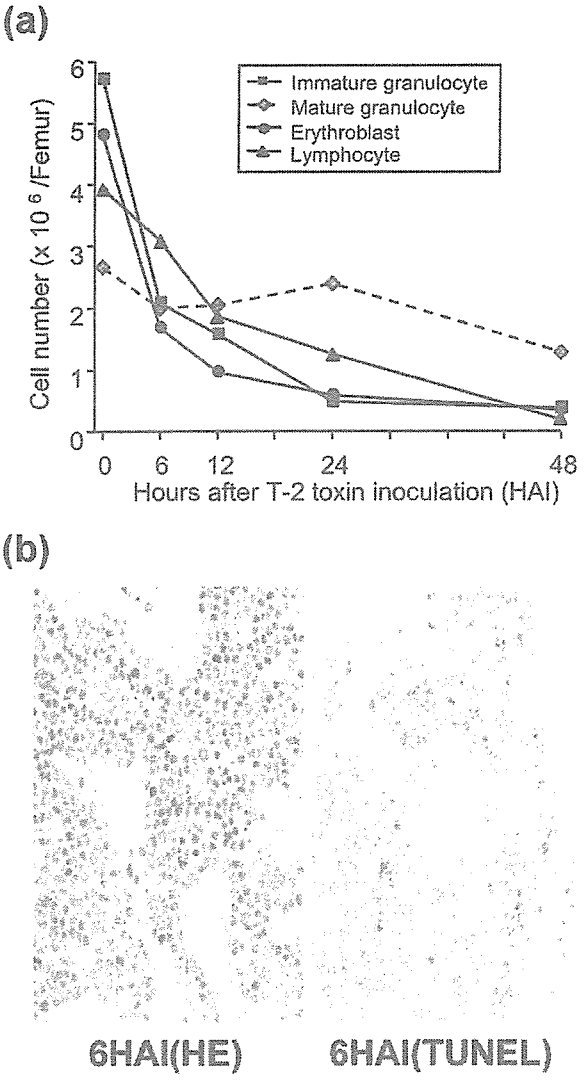

Fig. 4. Changes in differential myelocyte values (a) and histology (b) of femur bone marrow of mice after T-2 toxin treatment. Many pyknotic and TUNEL-positive cells are seen (b). (Shinozuka *et al.*, Toxicol Pathol. 26: 674–681. 1998 (modified)).

the largest lymphoid tissue in the circulation, and it is the site of erythrocyte storage and the removal of dysfunctional erythrocytes and leukocytes. In addition, it is well known that the red pulp of rodents has hematopoietic activity regardless of the age of the animals[30]. The splenic red pulp also shows a significant hypocellularity after T-2 toxin inoculation. The time of onset of the significant hypocellularity is similar between the bone marrow and the red pulp. In addition, apoptotic cells increase earlier in the red pulp than in the white pulp[27]. Similar difference in the onset of apoptosis is generally observed between hematopoietic and lymphoid tissues[31].

In vivo DNA and protein synthesis has been shown to be inhibited in the spleen, thymus, and bone marrow of mice given T-2 toxin[32], and some groups have reported a relationship between cytotoxic erythropoietic damage and a strong inhibition of the uptake of iron into erythropoietic cells in T-2 toxin-treated mice[33]. In addition, T-2 toxin has species-specific hemolytic effects on erythrocytes[34,35] and Gyongyossy-Issa and Khachatourians[36] have reported that T-2 toxin interacts with and binds to the membranes of spleen-derived lymphocytes from rodents. From these findings, it is speculated that T-2 toxin induces direct cytotoxicity to hematopoietic and lymphoid cells, resulting in the induction of apoptosis of these cells. In the bone marrow, damage to the hematopoietic microenvironments, i.e. degeneration of sinus endothelial cells and reticular cells and deposition of plasma proteins containing fibrinoid materials around degenerated sinuses[27], would also play an indirect role in the induction of apoptosis by T-2 toxin, because sinus endothelial cells and reticular cells are components of the hematopoietic microenvironments and play an important role in regulating hematopoiesis.

Lymphoid Tissues

In mice orally treated with T-2 toxin, the toxin attacks Peyer's patches first, then mesenteric lymph nodes, and finally the thymus in relation to the course of enteric absorption of orally inoculated T-2 toxin[37]. The degree of lymphocyte apoptosis is different among lymphoid tissues, including the splenic white pulp, and it is most prominent in the thymus, especially in its cortex, suggesting differences in the lymphocyte population susceptible to T-2 toxin among lymphoid tissues[25,37,38]. The weight and size of lymphoid tissues decrease due to the apoptosis of component lymphocytes.

It is reported that there is a difference in susceptibility to T-2 toxin among lymphocyte subsets. For example, in acute toxicity studies, $CD4^+CD8^+$ cells are the most sensitive to T-2 toxin[37,39,40] (Fig. 5). $CD44^{low}$ or $CD45^{low}$ cells, which are B lymphocyte precursor cells in the livers of fetal mice, are also highly susceptible[41]. Moreover, $CD44^{low}$ and $CD45^+$ cells in the bone marrow of adult mice are reduced after T-2 toxin-treatment[41].

In the thymus, $CD4^+CD8^+$ cells differentiate to $CD4^+CD8^-$ or $CD4^-CD8^+$ cells after coming in contact with dendritic cells which exist in the cortex[42], and this is responsible for the fact that apoptotic cells exist almost exclusively in the cortex. Between $CD4^+CD8^-$ cells and $CD4^-CD8^+$ cells, the former is more severely depressed[37] (Fig. 5). On the other hand, in a subacute toxicity study of T-2 toxin in mice, it was shown that $CD4^-CD8^-$ cells increased probably due to an accumulation of these cells due to an inhibitory effect of T-2 toxin on T cell differentiation[43].

In the mesenteric lymph nodes, $CD3^+$ cells are more clearly affected than $CD19^+$ cells, and the numbers of $CD4^+$ and $CD8^+$ cells are similarly decreased. In the Peyer's patches, the numbers of $CD3^+$, $CD19^+$ $CD4^+$ and $CD8^+$ cells are all similarly decreased. In addition, among IgM^+, IgG^+ and IgA^+ cells, the number of IgA^+ B cells, which are

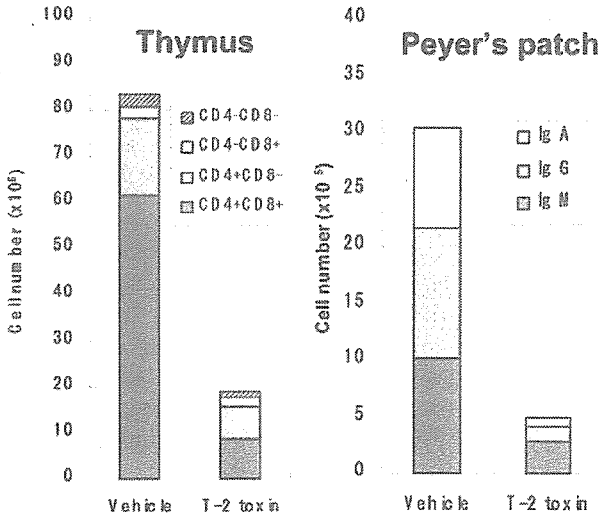

Fig. 5. Changes in mouse lymphocyte subsets at 24 hours after T-2 toxin treatment. (Nagata *et al.*, Exp Toxic Pathol. 53: 309–315. 2001 (modified)).

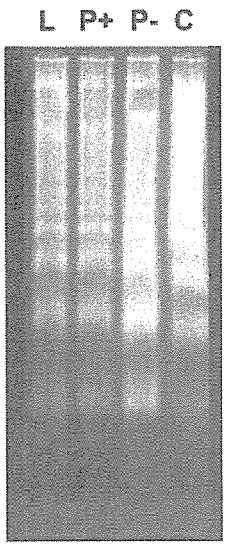

Fig. 6. Agarose gel electrophoresis of DNA extracted from thymus of mice at 24 hours after T-2 toxin treatment. L: *lpr/lpr* mouse, P+: *p53*+/– mouse, P–: p53–/– mouse, C: C57BL/6 mouse (wild type).

important in mucosal immunity, is most severely affected[37] (Fig. 5). IgA^+ B cells are highly expressed in the germinal centers during their differentiation in the Peyer's patches[44–46], and this may be at least partially related to the fact that apoptotic cells are seen almost exclusively in germinal centers.

Shinozuka *et al.*[47] have demonstrated that, among apoptosis-related genes (*fas*, *p53*, *bcl*, *c-myc*, and *c-fos*) examined by RT-PCR, the expression of *c-fos* mRNA is significantly elevated prior to the development of apoptosis

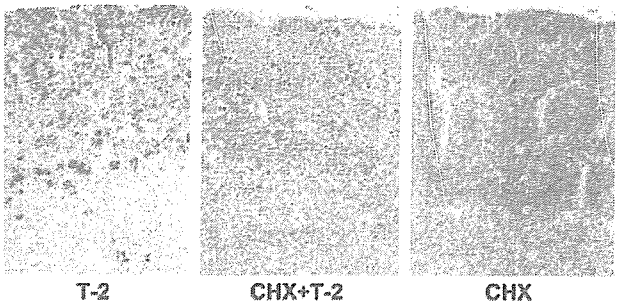

Fig. 7. Effect of pretreatment with protein inhibitor, cycloheximide (CHX), on T-2 toxin-induced apoptosis in thymus. TUNEL stain.

in the thymus of mice orally treated with T-2 toxin and that the elevation of *c-fos* mRNA and the development of apoptosis by T-2 toxin are not affected in p53-knockout mice or Fas-disfunctional *lpr/lpr* mutant mice (Fig. 6). Alam *et al.*[48] have also reported that T-2 toxin-induced apoptosis in thymocytes is independent of the Fas/Fas ligand pathway.

The activation of specific genes, including immediate-early response genes such as *c-fos*, *c-jun* and *c-myc*, is one of the early responses to acute cell injury[49,50]. Several studies have shown that the expression of *c-fos* mRNA precedes the initiation of apoptosis or is concomitant with apoptosis in many systems[51–53]. Colotta *et al.*[54] have shown that *fos* and *jun* are induced in the very early phase of apoptosis in hematopoietic cells after deprivation of growth factors and that blocking of these sequences by antisense oligonucleotides prevents apoptosis. Buttyan *et al.*[55] have reported that prostatic cell death after castration is accompanied by a sequential pattern of gene activity (*c-fos* → *c-myc* → *heat shock protein 70 (hsp70)*), and Preston *et al.*[56] have shown that the c-Fos induces apoptosis in sup-II preneoplastic cells in serum-free medium. In addition, they reported that c-FOS-induced apoptosis in their system is not blocked by cycloheximide, a protein inhibitor, suggesting that the transcriptional activation of *c-fos* is not involved in apoptosis of sup-II preneoplastic cells. On the other hand, cycloheximide suppresses apoptosis in the thymus of T-2 toxin-inoculated mice[47] (Fig. 7). Based on these findings taken together, the induction of *c-fos* mRNA is considered to be associated with T-2 toxin-induced apoptosis in lymphoid and hematopoietic tissues through apoptosis-related protein synthesis.

T-2 toxin also induces a rapid and continuous increase in the expression of *c-fos* mRNA prior to the development of apoptosis in ConA-stimulated mouse thymocyte primary cultures[57] (Fig. 8). Preincubation with BAPTA/AM, an intracellular calcium ion chelator, markedly suppresses the expression of *c-fos* mRNA and subsequent apoptosis by T-2 toxin (Fig. 9), suggesting that T-2 toxin-induced *c-fos* expression depends on $[Ca^{2+}]_i$. There is evidence that the regulation of *c-fos* expression involves a major intracellular second messenger, Ca^{2+} [58]. Similar involvement of $[Ca^{2+}]_i$

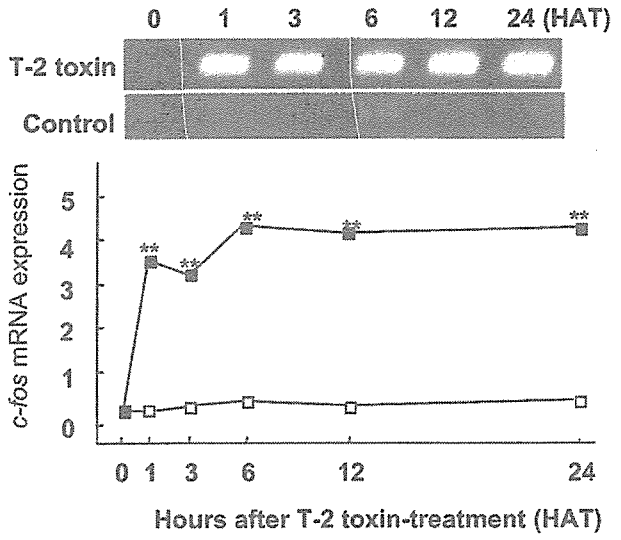

Fig. 8. Changes in *c-fos* mRNA expression in ConA-stimulated mouse thymocyte primary cultures after incubation with T-2 toxin. RT-PCR.

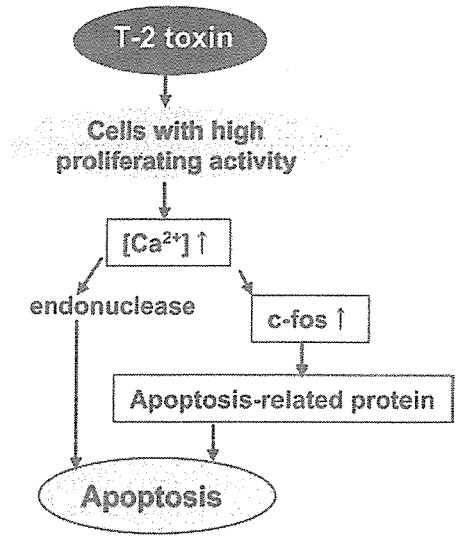

Fig. 10. Hypothesis of mechanisms involved in T-2 toxin-induced apoptosis in lymphoid tissues.

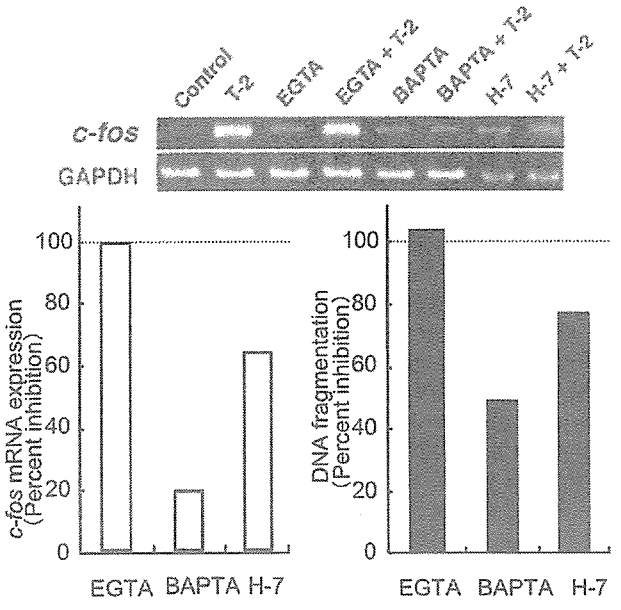

Fig. 9. Effects of calcium chelators and PKC inhibitor on T-2 toxin-induced *c-fos* mRNA expression and DNA fragmentation in ConA-stimulated mouse thymocyte primary cultures. EGTA: extracellular calcium chelator, BAPTA: intracellular calcium chelator, H-7: PKC inhibitor.

has been reported in the induction of *c-fos* after oxidative stress[59] and *hsp70* after heat shock[60]. Although the effect of T-2 toxin on $[Ca^{2+}]_i$ remains obscure, Yoshino *et al.*[61] have reported that the level of $[Ca^{2+}]_i$ is markedly elevated in HL-60 cells, a lymphoid cell line, after exposure to T-2 toxin. They have also reported that intracellular calcium chelators inhibit T-2 toxin-induced apoptosis in HL-60 cells. On the other hand, chelation of an extracellular ionized calcium ($[Ca^{2+}]_e$) by EGTA has no effect on the expression of *c-fos* mRNA or subsequent development of apoptosis in mouse thymocyte primary cultures after T-2 toxin-exposure[57] (Fig. 9), suggesting that the increase in $[Ca^{2+}]_i$ may not be due to the influx of extracellular Ca^{2+} but rather may be brought about by the intracytoplasmic release of Ca^{2+} from the endoplasmic reticulum.

Although less effective, preincubation with H-7, a protein kinase C (PKC) inhibitor, also significantly depresses the expression of *c-fos* mRNA and subsequent development of apoptosis (Fig. 9). These findings indicate that, in thymocyte primary cultures treated with T-2 toxin, *c-fos* may play an important role in the induction of apoptosis, and the increase in intracellular calcium may be closely related with the expression of *c-fos* mRNA. These findings also suggest that a PKC-dependent pathway may be involved in T-2 toxin-induced thymocyte apoptosis. In this regard, it is well known that both $[Ca^{2+}]_i$ mobilization and PKC activation lead to an increase of *c-fos* transcription[58,62]. In addition, it is also reported that the induction of apoptosis in HK-60 cells by T-2 toxin involves activation of caspase-3 and -9 through the release of cytochrome c from mitochondria in the cytosol[63]. A recent study on gene expression profiles by Shinozuka *et al.* showed that the early up-regulation of the *c-jun* gene was also detected by microarry analysis in lymphoid tissues of mice treated with T-2 toxin, of which the data will be published elsewhere.

The above-mentioned *in vivo* and *in vitro* findings suggest that the *c-fos* gene plays an important role in the early phase of T-2 toxin-induced apoptosis probably through the synthesis of a certain protein, and the elevation of *c-fos* mRNA expression may require the mobilization of $[Ca^{2+}]_i$

and partially involve a PKC-dependent pathway (Fig. 10). The mobilization of $[Ca^{2+}]_i$ seems to activate calcium-dependent enzymes, resulting in internucleosomal DNA fragmentation. T-2 toxin-induced apoptosis in hematopoietic and lymphoid tissues is considered to be independent of the Fas/Fas ligand pathway and p53-related pathway.

Gastrointestine

In mice treated orally with T-2 toxin, apoptosis occurs earlier in the intestine than in the stomach. In the stomach, apoptosis develops first in surface epithelial cells, and then extends to the chief cells of the glandular stomach, when apoptosis starts in the basal layer of the forestomach[64]. Parietal cells in the glandular stomach are almost free from apoptosis, though they shows dilatation of intracellular canaliculi and vacuolation (Fig. 11).

In the intestine, apoptosis is exclusively found in crypt epithelial cells[64,65] (Fig. 11) and lymphoid cells in the lamina propria and Peyer's patches[37,66]. The apoptotic index of crypt epithelial cells begins to increase simultaneously in all regions examined (duodenum, ileum, cecum and colon), and it is markedly higher in the small intestine than in the large intestine. This difference in the apoptotic index between the small and large intestines may be related to the repeated exposure of the small intestine to T-2 toxin and its metabolites through mucosal absorption and biliary excretion *via* the enterohepatic circulation[18].

The mitotic index begins to drastically decrease when the apoptotic index starts to increase, and thereafter both indices gradually returns to the control levels with the passage of time. However, the apoptotic index after T-2 toxin inoculation is not always proportional to the mitotic index before T-2 toxin inoculation[64]. In addition, there are clear mouse strain- and sex-differences in the apoptotic index but not in the mitotic index[65]. These findings suggest that the suppression of mitotic activity by T-2 toxin may not be a direct cause of the increase in apoptosis in the crypt epithelium after T-2 toxin treatment.

Dorsal Skin

T-2 toxin penetrates through the skin[67–69], and some researchers have reported that T-2 toxin causes local[70,71] as well as generalized injuries[72,73] upon topical application to the dorsal skin. This seems to be important because there is a chance that the skin of grain-handling workers as well as of domestic animals would be exposed to T-2 toxin-contaminated grain dust.

Albarenque *et al.* have carried out a series of experiments of acute dorsal skin lesions up to 24 hours (24 hr) after topical application of T-2 toxin to the dorsal skin of Wistar-derived hypotrichotic WBN/ILA-*Ht* rats (HtR), which have an autosomal dominant gene (*Ht*: dominant hypotrichotic) responsible for the characteristics of hypotrichosis[74]. In the epidermis, basal cell proliferating activity evaluated by the number of proliferating cell nuclear antigen (PCNA)-positive cells is first suppressed, and basal cell apoptosis develops later (Fig. 12). In the dermis, inflammatory responses, including mast cell infiltration, start when the suppression of basal cell proliferating activity begins, and they are followed by capillary endothelial degeneration, edema and an increase in the numbers of mast cells and fibroblasts[75].

As for apoptosis-related genes (*p53*, *bcl-2*, *c-ki-ras*, *c-fos* and *c-jun*) examined by the RT-PCR method, the expression of *c-fos* mRNA markedly increases prior to the development of epidermal basal cell apoptosis (Fig. 13). Although not prominent, the expression of *c-jun* mRNA also shows a significant elevation concomitant with the elevation of *c-fos* expression[76] (Fig. 13). As mentioned before, *c-fos* is a kind of immediate-early response genes, and its activation together with that of other factors such as *c-jun* occurs as an early respose to cell injury, resulting in an increase in the sensitivity of keratinocytes to apoptosis[77]. Thrichothecene mycotoxins trigger ribotoxic stress response activating JNK/p38[78], and JNK/p38 stimulates immediate-early response genes, *c-fos* and *c-jun*, both of which encode components of transcription factor AP-1[79].

In addition, among the mRNAs of such cytokines as TGF-β_1, TNF-α, IL-1α, IL-1β, IL-6 and IL-10 examined after topical application of T-2 toxin, the level of TGF-β_1 mRNA of the whole skin tissue is elevated slightly from the early phase, and then reaches a significantly higher level later[80] (Fig. 13). Such changes in the level of TGF-β_1 mRNA following T-2 toxin treatment correspond well to the time course of the induction of basal cell apoptosis. In this connection, it has been reported that human keratinocytes could undergo apoptosis after growth arrest under the effect of TGF-β_1[81]. In addition, the depression of epidermal basal cell proliferating activity becomes more prominent in accordance with the clear elevation of the TGF-β_1 mRNA level, suggesting that TGF-β_1 may have a relationship to the depression of epidermal basal cell proliferating activity[75,80].

In the T-2 toxin-treated skin, signals of TGF-β_1 mRNA detected by *in situ* hybridization method begin to increase first in the epidermis, and they increase much more in both the epidermis and dermis later, and clear increases in the signal of TGF-β_1 correspond well to the elevation of TGF-β_1 mRNA[80]. It is also known that the elevated expression of TGF-β_1 mRNA may act as one of the chemoattractants for mast cells[82] and fibroblasts and as a stimulator for fibroblast proliferation[83,84]. These alterations are responsible for the above-mentioned changes in the dermis after topical application of T-2 toxin[75].

Following the topical application of T-2 toxin to the dorsal skin, the level of TNF-α mRNA also shows a marked elevation from the early to late phase, and that of IL-1β mRNA shows a slight but significant elevation simultaneously[85] (Fig. 13). The possible role of TNF-α as an apoptosis-inducer has been reported in various kinds of cells, including keratinocytes[86,87]. Meng *et al.*[88] have suggested that TNF-α can interact with its receptors, and signals from

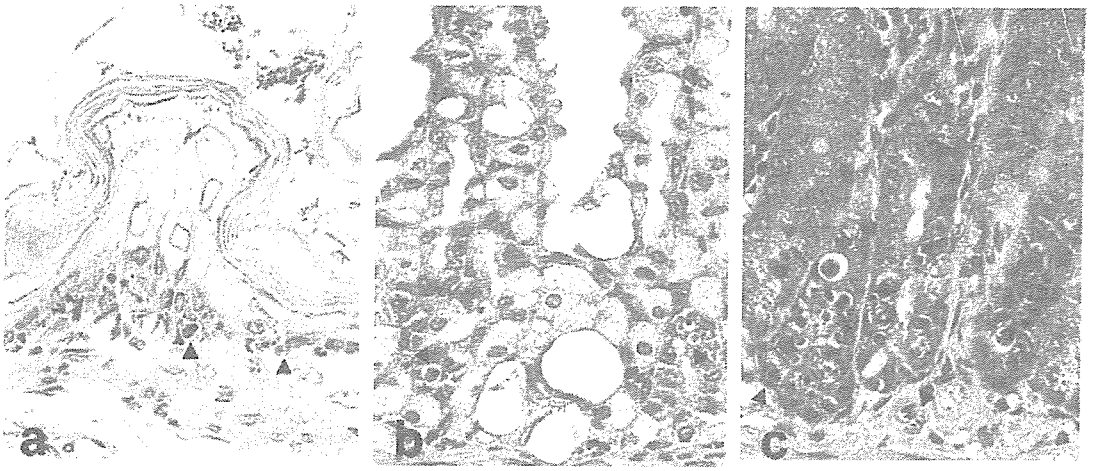

Fig. 11. Histology of the gastrointestine (a: forestomach, b: glandular stomach, c: duodenum) of mice after T-2 toxin treatment. Pyknotic cells (arrowheads) are seen. HE stain.

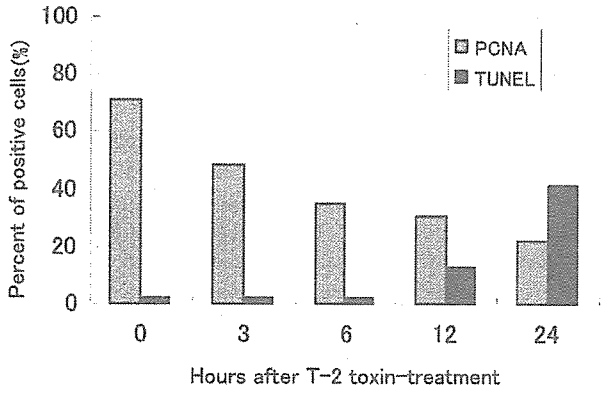

Fig. 12. Changes in the percentage of PCNA- or TUNEL-positive epidermal basal cells after topical application of T-2 toxin to the dorsal skin of WBN/ILA-*Ht* rats. (Albarenque *et al.*, Histol Histopathol. 14: 337–342. 1999 (modified)).

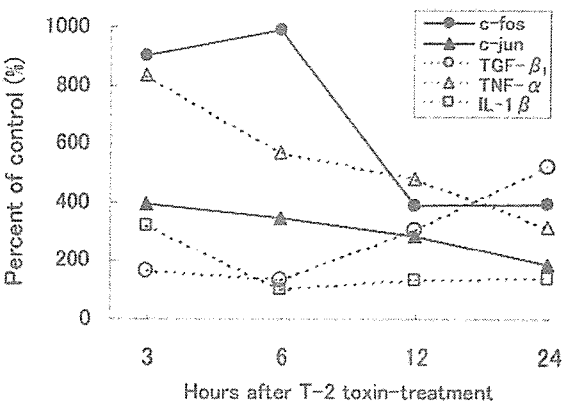

Fig. 13. Changes in the expression of *c-fos*, *c-jun*, TGF-β_1, TNF-α and IL-1β mRNAs after topical application of T-2 toxin to the dorsal skin of WBN/ILA-*Ht* rats.

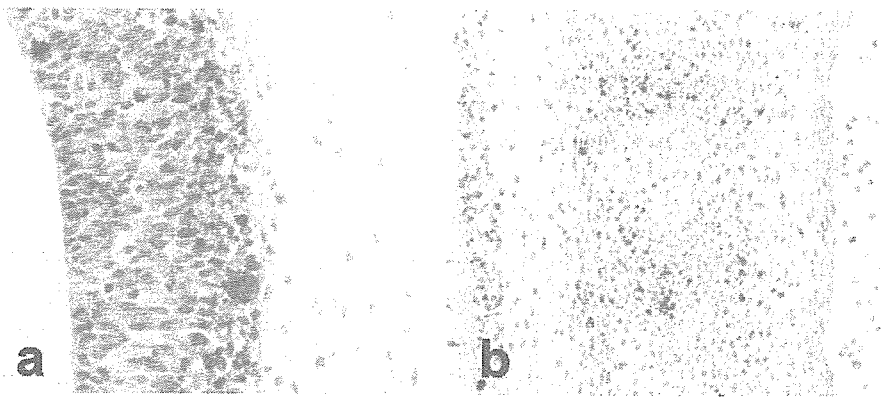

Fig. 14. TUNEL-positive apoptotic cells in the telencephalon (a) and caudal sclerotomic segment (b) of fetuses from pregnant mice treated with T-2 toxin on day 11 of gestation.

these receptors have relationships with the induction of some genes such as *c-myc*, *c-fos* and *caspase*, resulting in the induction of apoptosis[89]. It is also known that keratinocytes can release proinflammatory cytokines, such as TNF-α and IL-1β, when they are injured[90]. In addition, it has been demonstrated that keratinocytes are directly activated by exogenous stimuli[90,91] and, after abrogation of the barrier, epidermal cells respond by producing various molecules, including TGF-β_1 and TNF-α[92].

As in the case of *in vivo* experiments[76,80,85], the expression of apoptosis-related genes (*c-fos* and *c-jun*) and the mRNAs for cytokines (TNF-α and IL-1β)markedly increases prior to the development of apoptosis in rat keratinocyte primary cultures exposed to T-2 toxin[93].

Judging from the above-described *in vivo* and *in vitro* findings, it is considered that the induction of TNF-α and TGF-β_1 mRNAs as well as that of *c-fos* and *c-jun* may have a close relationship with T-2 toxin-induced epidermal basal cell apoptosis.

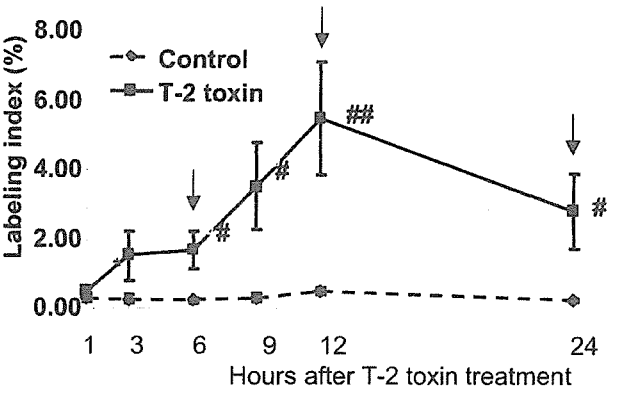

Fig. 15. Changes in the TUNEL labeling index in the rat fetal telencephalon after T-2 toxin treatment to dams on day 13 of gestation. ↓: time point of microarray analysis. (Sehata *et al.*, Food Chem Toxicol. 42: 1727–1736. 2004 (modified)).

Fetal Tissues

T-2 toxin readily crosses the placenta, is distributed to the fetal tissues[94] and induces fetal death, necrosis of the fetal brain and fetal bone malformations[95]. In addition, thymic atrophy and decreases in the viability of hematopoietic progenitor cells in the liver and in the number of B cells have also been reported in fetuses from dams exposed to T-2 toxin[41,43]. Moreover, changes attributable to T-2 toxin-treatment have been reported in the nervous system, liver, gastrointestinal tract and cartilage primordium in rat fetuses[96,97]. Bone malfomations such as incomplete ossification, absence of bones, wavy bones and fused bones[95,98–100] may be related to the induction of apoptosis in the caudal half of the sclerotome around the notochord, and in the mesenchyme, chondroblasts and chondrocytes around the cartilage primordium detected in fetuses from dams treated with T-2 toxin[101].

Ishigami *et al.*[102] first reported that T-2 toxin could induce apoptosis especially in the central nervous and skeletal systems after oral administration of T-2 toxin to pregnant mice (Fig. 14), and they demonstrated that T-2 toxin-induced skeletal malformations and apoptosis in the fetal telencephalon are greatly reduced by pretreatment with cyclohexamide. In addition, the number and region of apoptotic cells in the mouse fetuses vary according to the administration date. For example, apoptosis is observed in many neuroepithelial cells and a small number of chondroblasts and chondrocytes on embryonic day 13.5 while it is detected in many cells in the thymus and renal subcapsular parencyma on embryonic day 16.5[101].

T-2 toxin is generally considered to induce apoptosis in actively proliferating cells in embyos and fetuses, probably through its radiomimetic effect, as observed in lymphoid and hematopoietic tissues. However, it should not be forgotten that a small number of TUNEL-positive cells are also observed in some regions where PCNA-positive cells are not detected[101], suggesting that T-2 toxin-induced apoptosis in the developing mouse fetus might also be affected by some other factors in addition to the proliferating activity of the target cells.

Sehata *et al.*[97] have investigated the mechanisms of T-2 toxin-induced apoptosis in the fetal brain by the oral administration of T-2 toxin to pregnant rats on day 13 of gestation. The number of apoptotic neuroepithelial cells in the telencephalon increases at 1 hr and peaks at 12 hr[97] (Fig. 15). As mentioned above, T-2 toxin passes through the placenta[94], and the blood brain barrier is not completely developed before embryonic day 18 in rats[103]. In addition, T-2 toxin and its metabolite HT-2 have a lipophilic nature and the fetal brain is rich in lipids. Therefore, T-2 toxin may be easily distributed to the fetal brain.

Microarray analysis done on the fetal brain at 6, 12 and 24 hr has revealed that the expression of oxidative stress-related genes (*hsp70, metallothionein (MT)-2* and *-1* and *heme oxygenase (HO)-1*) is strongly induced by T-2 toxin at 12 hr, the peak time of apoptosis induction, and the expression of the Cu, Zn-superoxide dismutase (Cu, Zn-SOD) gene also increases later[97]. The expression of mitogen-activated protein kinase (MAPK)-related genes (*MEKK1* and *c-jun*) and other apoptosis-related genes (*caspase-2, insulin-like growth factor-binding protein-3 (IGF-BP3), tissue inhibitors of metalloproteinase (TIMP)-3*) is also induced by T-2 toxin treatment[97] (Fig. 16). Data of real time RT-PCR analysis done on *HSP70* and *HO-1* genes have shown a good correlation with those of microarray analysis[97] (Fig. 17).

It is known that oxidative stress induces the elevation of *HSP70, HO, MT* and *CuZn-SOD* gene expression[104–107], resulting in apoptosis in the nervous system[108]. This suggests that T-2 toxin is able to induce oxidative stress and subsequent apoptosis in the fetal brain, as reported in the dam's liver, placenta and fetal liver in pregnant rats treated with T-2 toxin[109].

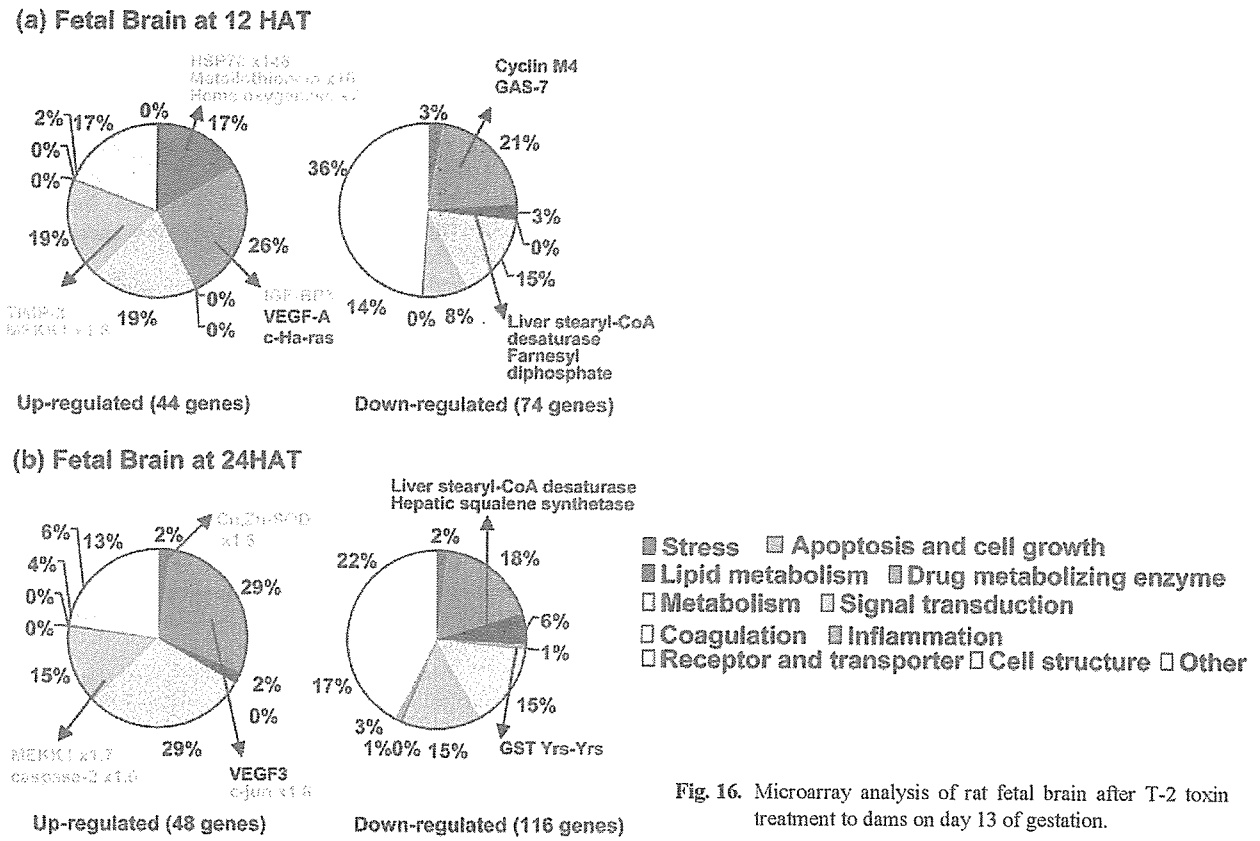

Fig. 16. Microarray analysis of rat fetal brain after T-2 toxin treatment to dams on day 13 of gestation.

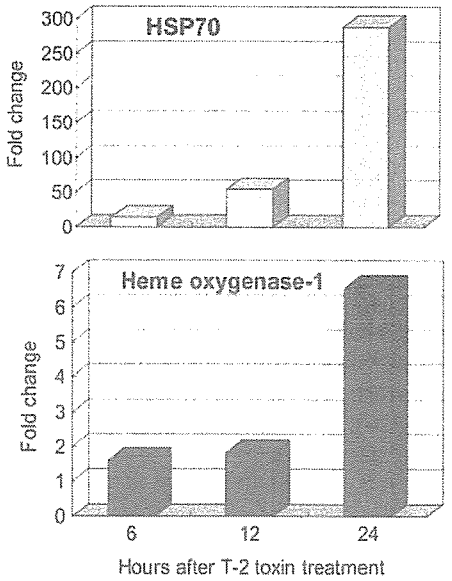

Fig. 17. Changes in the expression of *HSP70* and *heme oxygenase-1* mRNAs in the rat fetal brain after T-2 toxin treatment to dams on day 13 of gestation. Real-time RT-PCR.

MAPKs are important intermediates in signaling pathways for responding to extracellular stress. For example, extracellular signal-related protein kinase (ERK) mediates cell growth and protects cells from apoptosis, wherease stress-activated protein kinase (SAPK)/c-Jun N-terminal kinase (JNK) and p38 MAPK inhibit cell proliferation and may promote apoptosis[110]. Each MAPK is activated by an upstream MAPK kinase including MEKK1, and activates transcription factors such as *c-jun* and *c-fos*. MEKK1 may induce apoptosis by causing a general deregulation of MAP kinase signaling[111]. It is also reported that JNKs and c-Jun are important regulators of apoptosis in the nervous system[112]. In addition, it is reported that T-2 toxin and other trichothecene mycotoxins induce apoptosis by activating MAPKs[113,114], and increased expression of *c-fos* and *c-jun* genes has been reported in the skin topically treated with T-2 toxin[76]. Therefore the MAPK-JNK-c-Jun pathway is considered to be involved in T-2 toxin-induced apoptosis in the fetal brain.

It is known that TIMP-3 induces a type II apoptotic pathway initiated *via* a Fas-associated death domain-dependent mechanism[115] and the expression of *TIMP-3* is elevated in the fetal brain treated with T-2 toxin[97]. In addition, as mentioned above, TNF-α is involved in T-2 toxin-induced epidermal basal cell apoptosis[85]. Therefore there is a possibility that the TNF receptor pathway may also be involved in the mechanisms of T-2 toxin-induced apoptosis in the rat fetal brain.

Caspase activation is known to play an important role in the induction of apoptosis[116]. The activation of caspase-2 (but not of caspase-9 or 3), which has been detected in the T-